Rare earth element distribution on the Fuerteventura Basal Complex (Canary Islands, Spain): a geochemical and mineralogical approach

Marc Campeny[1], Inmaculada Menéndez[2], Luis Quevedo[2,3], Jorge Yepes[2], Ramón Casillas[4], Agustina Ahijado[4], Jorge Méndez-Ramos[3], José Mangas[2]

[1] Departament de Mineralogia, Museu de Ciències Naturals de Barcelona, Passeig Picasso s/n, 08003 Barcelona, Spain
[2] Instituto de Oceanografía y Cambio Global, IOCAG, Universidad de Las Palmas de Gran Canaria, 35017 Las Palmas de Gran Canaria, Spain
[3] Instituto de Materiales y Nanotecnología, Departamento de Física, Universidad de La Laguna, apartado correos 456, 38200 La Laguna, Tenerife, Spain
[4] Departamento de Biología Animal, Edafología y Geología, Universidad de La Laguna, apartado correos 456, 38200 La Laguna, Tenerife, Spain.

Correspondence to: Marc Campeny (mcampenyc@bcn.cat)

Abstract. The Fuerteventura Basal Complex comprises of Oligocene and Miocene ultra-alkaline-carbonatitic magmatic pulses with outcrops that extend across kilometre-scale areas in some specific sectors of this oceanic island. Additionally, there is evidence of associated weathering materials that affect these magmatic lithologies. These alkaline magmatic rocks (including trachytes, phonolites, syenites, melteigites, and ijolites), carbonatites, and their associated weathering products underwent a preliminary evaluation of REE contents based on mineralogical and geochemical studies. REE concentrations in carbonatites of about 10,300 ppm REY (REEs plus yttrium) have been detected, comparable to other locations hosting significant deposits of these critical elements worldwide. Conversely, alkaline magmatic rocks and the resulting weathering products display limited REE contents. Notably, REEs in carbonatites are associated with primary accessory phases such as REE-bearing pyrochlore and britholite, and secondary monazite. The results obtained in the carbonatites of Fuerteventura underscore the interest in studying the concentrations of critical elements, such as REEs, within a non-conventional geological setting like oceanic islands. However, due to intricate structural attributes, the irregular distribution of these mineralizations, and possible land use and environmental constraints, additional future detailed investigations are imperative to ascertain the real potential of these REE concentrations.

Keywords. Fuerteventura, Canary Islands, Oceanic Island, Rare earth elements, Carbonatites

1 Introduction

The European Commission (EC) is spearheading efforts to combat climate change through the European Green Deal (EGD), with the goal of achieving a carbon-neutral continent by 2050 (European Commission, 2019). This initiative entails transitioning to green technologies, which heavily rely on rare earth elements (REEs) for applications like renewable energy systems and electric vehicles. (Acosta-Mora et al., 2018; Alonso et al., 2012; Chakhmouradian and Wall, 2012; Massari and Ruberti, 2013; Méndez-Ramos et al., 2013; Wondraczeck et al, 2015).

According to the International Union of Pure and Applied Chemistry (IUPAC), REEs comprise a group of 17 chemical elements: scandium (Sc), yttrium (Y) and the 15 members of the lanthanide series (Connelly et al., 2005). The term "rare" is confusing because, even though REEs seldom occur in pure mineral phases, their average concentration in the Earth's crust is around 125 ppm, surpassing other metals such as copper, gold or platinum (Long et al., 2010; Rudnick and Gao, 2014).

Given their pivotal role in modern industry and green technologies, as well as the projected increase in demand for REEs in the coming years, governments worldwide are actively promoting the advancement of knowledge regarding REE distribution in the geological environment (Barteková and Kemp, 2016; European Commission, 2023a; European Commission, 2023b).

The study of REEs has primarily centred on investigating non-conventional HREE geological settings such as soils and weathering products (Braun et al., 1993; Wang et al., 2010, Wang et al., 2013; Berger et al., 2014; Aiglsperger et al., 2016; Torró et al., 2017; Reinhardt et al., 2018; Borst et al., 2020), but also traditional and well-known LREE-bearing lithologies, such as carbonatites (Goodenough et al., 2016; Yang et al., 2019; Pirajno and Yu, 2022).

Carbonatites are igneous rocks formed by carbonate mantle melts and are genetically associated with a wide range of mafic, ultramafic, and alkaline silicate rocks (Yaxley et al., 2002). Although carbonates such as calcite or dolomite are their main forming minerals, a significant portion of carbonatites contain accessory phases enriched in critical metals such as REEs (Christy et al., 2021). REEs can be contained in fluorcarbonates (e.g., bastnäsite, parisite, huanghoite, synchysite), phosphates (e.g., monazite, rhabdophane), silicates (e.g., allanite), or even oxides (e.g., REE-bearing pyrochlore, cerianite). These accessory minerals make carbonatites the main current REE source, representing 86.5% of the deposits under exploitation for these elements (Liu et al., 2023). However, although carbonatites are rare rocks, predominantly found in continental rifts associated with cratons (Humphreys-Williams et al., 2021), they

have exceptionally been described in other geological contexts, most notably oceanic islands associated with hotspots, such as Cape Verde (Mourão et al., 2010; De Ignacio et al., 2018;) or Fuerteventura in the Canary Islands (Mangas et al., 1996; Carnevale et al., 2021).

The petrogenesis of carbonatites is still a debated topic (Anenburg et al., 2021; Yaxley et al., 2022). Different processes have been proposed for their formation, although there is a consensus that they originate from primary fusion processes derived from a carbonated mantle (Kamenetsky et al., 2021). For the specific case of the oceanic carbonatites, this debate is even more lively. Doucelance et al. (2010) suggested a shallow origin from low-degree partial melting at the base of the oceanic lithosphere. Other authors have proposed the involvement of unmixing process linking to alkaline magma suites (Weidendorfer et al., 2016), the action of hydrothermal fluids of marine origin enriched in Ca that would have serpentinized the mantle (Park and Rye, 2013) or even the contribution of recycled marine carbonates through subduction or assimilated in shallow magma chambers (Démeny et al., 1998; Hoernle et al., 2002; Doucelance et al., 2014).

The present study focuses on the mineralogical and geochemical analysis of carbonatites and associated alkaline igneous rocks, as well as their weathering products, in three distinct sectors in the western region of Fuerteventura (Canary Islands, Spain; see Figure 1). The primary objective of this research is to deepen our understanding of REE distribution in these materials, within the exotic geological context of an oceanic island associated with intraplate magmatism.

2 Geological setting

2.1 The Canary Island Seamount Province

The Canary Islands archipelago, located between 27°N and 30°N of latitude, is part of the Canary Island Seamount Province (CISP). This volcanic region forms a band of approximately 1300 km in length and 350 km in width, running parallel to the African continental margin. Within the CISP, there are over 100 seamounts and up to 8 emerged islands: El Hierro, La Palma, La Gomera, Tenerife, Gran Canaria, Lanzarote, Fuerteventura and Savage islands (Courtillot et al., 2003; Schmincke and Sumita, 2010; van den Bogaard, 2013). Based on magnetic anomaly measurements and dating of both emerged and submarine igneous materials, volcanic activity in the CISP spans more than 142 Ma, from the Early Cretaceous to the present day (Frisch, 2012; van den Bogaard, 2013; Longpré and Felpeto, 2021).

2.2 Fuerteventura Island

Fuerteventura, the easternmost island of the Canarian archipelago, along with Lanzarote, forms the emergent crest of the Eastern Canarian Volcanic Ridge, which is located approximately 100 km offshore from the Moroccan coast (Figure 1). Fuerteventura is the oldest island in the archipelago, with its initial stages of formation linked with submarine volcanic activity, dating to the Oligocene (~34 Ma). The first episodes of subaerial volcanism occurred around ~23 Ma (Coello, 1992; Ancochea et al., 1996; Pérez-Torrado et al., 2023).

Fuerteventura is characterized by the occurrence of three distinct main geological units, arranged in order from oldest to youngest: the Fuerteventura basal complex (FBC), the Miocene subaerial volcanic units, and the Pliocene-Quaternary volcano-sedimentary facies (Fúster et al., 1968; Le Bas et al., 1986; Muñoz et al., 2005; Gutiérrez et al., 2006; Troll and Carracedo, 2016).

2.2.1 The Fuerteventura basal complex

The FBC unit mainly outcrops in the western part of the island (Figure 1). Two different groups of lithofacies may be distinguished: (1) Early Jurassic to Late Cretaceous oceanic crust materials (Steiner et al., 1998), constituted by mid-ocean ridge basalts and oceanic sediments; (2) Oligocene submarine and transitional volcanic rocks associated with plutonic bodies and dyke swarms (Feraud et al., 1985; Hobson et al., 1998; Gutiérrez et al., 2006). In this second group, a set of lithologies can be distinguished related to an ultra-alkaline-carbonatitic magmatic pulse that occurred ~25 Ma (Le Bas, 1981; Barrera et al., 1986; Balogh et al., 1999). Additionally, alkaline ultramafic, mafic and felsic plutonic rocks such as wehrlites, pyroxenites, gabbros and syenites intruded the previously existing Oligocene materials, forming distinctive ring complexes (Muñoz et al., 2005). These magmatic rocks, predominantly of Oligocene age, have been interpreted as episodes of submarine and transitional growth in Fuerteventura (Le Bas et al., 1986; Gutiérrez et al., 2006).

In general, outcrops related with the FBC intrusive assemblage exhibit significant variations and four distinct morphologies and characteristic textures can be identified (Fúster et al., 1968; Barrera et al., 1986; Le Bas et al., 1986; Fernández et al., 1997; Mangas et al., 1992, 1994, 1997; Ahijado 1999; Ancochea et al., 2004; Ahijado et al., 2005; Muñoz et al., 2005):

(1) Basaltic, alkaline and carbonatitic dykes and veins of meter-scale, decimeter-scale, and centimeter-scale, that are randomly distributed, resulting in a chaotic arrangement (Figure 2a, b). Related to the carbonatite veins and dikes, an intense fenitization may occur.

(2) Shear zones (Fernández et al., 1997), characterized by gradual or diffuse boundaries, which display assimilation structures between different rock bodies, along with the presence of mylonites, and brecciated textures resulting from deformation (Figure 2c).

(3) Pegmatitic textures developed within certain rock bodies, often containing centimeter-sized crystals of rock-forming minerals (Figure 2d).

(4) Contact metamorphism and metasomatism, as well as skarn zones that occur in deformed or undeformed carbonatites, influenced by subsequent hydrothermal fluid circulation (Ahijado et al., 2005; Casillas et al., 2008, 2011).

In addition, during Miocene magmatic pulses, alkaline plutons were formed in the central-western part of Fuerteventura Island north of the locality of Pájara (sector 2, Figure 1). These intrusions constitute typical ring complexes of alkaline magmatic rocks, including nepheline syenites, syenites, and trachytes (Muñoz, 1969). They are regarded as the most recent rocks in the FBC (Figure 1) and have been dated using the K-Ar method, yielding an approximate age of 20.6 ± 1.7 Ma (Le Bas et al., 1986; Holloway and Bussy, 2008).

2.2.2 Miocene subaerial volcanic unit

During the Miocene, Fuerteventura witnessed the formation of up to three volcanic edifices (Figure 1; Coello et al., 1992; Ancochea et al., 1996). The northern volcanic structure, referred to as the Tetir edifice, experienced two volcanic construction phases between 22 and 12.8 Ma (Balcells et al., 1994). These episodes involved the eruption of basalts, picritic basalts, oceanic basalts, trachybasalts and trachytes. In the central part of the island, the Gran Tarajal edifice developed three different construction phases spanning from 22.5 to 14.5 Ma (Balcells et al., 1994). On the Jandía Peninsula, in the southern part of the island, a volcanic edifice comprising both basaltic and trachybasaltic materials emerged. It formed three successive construction episodes occurring between 20.7 and 14.2 Ma ago (Balcells et al., 1994). Based on their mineralogical and petrological features, the lithologies comprising this unit have not been considered as potentially containing significant concentrations of REEs. Therefore, they have not been included in the present study.

2.2.3 Pliocene and Quaternary volcano-sedimentary facies

After the subaerial volcanic activity during the Miocene, a period of volcanic quiescence ensued, leading to the erosion of the previously formed volcanic edifices. Subsequently, during the Pliocene (between 5.3 and 2.6 Ma), a phase of magmatic rejuvenation began, characterized by scattered Strombolian eruptions (Figure 1). Concurrently, various sedimentary formations emerged across the entire island, including littoral and shallow-water marine deposits, as well as aeolian, colluvial, and alluvial subaerial sediments and paleosols from the Pliocene to the Quaternary (Fúster et al., 1968; Zazo et al., 2002; Ancochea et al., 2004). The soils on Fuerteventura are predominantly classified as eutric cambisols and lithosols-vitric andosols, according to the FAO/UNESCO (1970) nomenclature. However, the current arid and deforested conditions have led to extensive erosion of the weathered rock profiles present in different areas of the island. Edaphic calcretes are abundant in Fuerteventura (Alonso-Zarza and Silva, 2002; Huerta et al., 2015), with their primary source of calcium believed to be the Pliocene paleodunes formed by calcarenites, rather than the parent igneous rock itself (Chiquet et al., 1999; Huerta et al., 2015; Alonso-Zarza et al., 2020). Interestingly, the aeolian dust deposits predominantly originate from the Sahara Desert (Goudie and Middleton, 2001; Menéndez et al., 2007; Scheuvens et al., 2013).

3 Materials and Methods

3.1 Sampling

Alkaline magmatic rocks and especially carbonatites are considered potential targets for the exploration of rare earth elements (Goodenough et al., 2016; Balaram et al., 2019; Anenburg et al., 2021; Beland and Jones, 2021). In Fuerteventura, these types of lithologies are found in two distinct geological areas: the Oligocene (sectors 1 and 3; Figure 1) and the Miocene lithologies related with the FBC (sector 2, Figure 1).

Considering that weathering profiles may concentrate REE in larger quantities than primary bedrocks (Bao and Zhao, 2008; Menéndez et al., 2019, Braga and Biondi, 2023; Chandler et al., 2024), these lithological formations were included in the present study and sampling was conducted on a selection of six different

184 profiles: (1) Agua Salada ravine (sector 1) and (2) Aulagar ravine (sector 3), developed on carbonatites, (3)
185 the FV-30 road, (4) Las Peñitas quarry, (5) Palomares ravine and (6) the Pájara profiles, on syenite bedrock
186 (Figure 1; Table S1).
187 Accordingly, a systematic sampling campaign was conducted in three different sectors of Fuerteventura,
188 targeting alkaline and carbonatitic igneous rocks and their associated weathering products. The specific
189 locations of these predetermined sectors are outlined in Figure 1. As a result, a set of 29 representative
190 samples of potentially REE-enriched magmatic rocks, along with 21 samples of associated weathering
191 products, were collected for further analysis (Table S1). For the weathering products, we conducted six
192 sampling profiles (labelled A to F; Figure 1) at various suitable points to compare the mineralogical and
193 geochemical changes resulting from weathering of the primary magmatic rocks.
194

195 **3.2 Petrographic and mineralogical studies**

196 Selected samples of magmatic rocks were prepared in thin sections for textural and mineralogical analysis
197 at the Laboratory of Geological and Paleontological Preparation of the Natural Sciences Museum of
198 Barcelona (LPGiP-MCNB; Barcelona, Spain). A representative subset of these samples was also examined
199 using a JEOL JSM-7100 field emission scanning electron microscope (FE-SEM) at the Scientific and
200 Technological Centers of the Universitat de Barcelona (CCiTUB). The FE-SEM system is equipped with
201 an INCA Pentaflex EDS (energy dispersive spectroscopy) detector (Oxford Instruments, England), which
202 allowed for the acquisition of semi-quantitative analyses of mineral phases. The general operating
203 conditions for the FE-SEM were a 15-20 kV accelerating voltage and a 5 nA beam current.
204 To achieve accurate and precise mineralogical identification and characterization of the weathering
205 magmatic rocks and calcretes, X-ray powder diffraction (XRPD) measurements were performed using a
206 PANalytical Empyrean powder diffractometer equipped with a PIXcel1D Medipix 3 detector at the
207 Integrated XRD Service of the General Research Support Service of La Laguna University, Spain. The
208 diffractometer employed incident Cu K_α radiation at 45 kV and 40 mA, along with an RTMS (real-time
209 multiple strip) PIXcel1D detector with an amplitude of 3.3473° 2θ. The diffraction patterns were obtained
210 by scanning random powders in the 2θ range from 5° to 80°. Data sets were generated using a scan time of
211 57 seconds and a step size of 0.0263° (2θ), with a 1/16° divergence slit. Mineral identification and semi-
212 quantitative results were obtained using the PANalytical's HighScore Plus search-match software (v. 4.5)
213 with a PDF+ database.

3.3 Geochemical analyses

The major elements composition of carbonates from carbonatites was studied using an electron probe microanalyzer (EPMA) system. The EPMA analyses were conducted on a JEOL JXA-8230 electron microprobe, equipped with five wavelength-dispersive spectrometers and a silicon-drift detector EDS, located at the CCiTUB. The spot mode was employed for the analyses and the electron column was set to an accelerating voltage of 15 kV and a beam current of 10 nA. Standard counting times of 10 seconds were used, along with a focused beam, to achieve the highest possible lateral resolution. The analytical standards employed during the analysis process were: celestine (PETJ, Sr K_α) wollastonite (PETL, Ca K_α), periclase (TAPH, Mg K_α), hematite (LiFH, Fe K_α), rhodonite (LiFH, Mn K_α) and albite (TAPH, Na K_α).

Bulk-rock geochemical data of major and trace element composition were obtained by X-ray fluorescence (XRF) and inductive coupled plasma (ICP)-emission spectrometry. The samples were prepared by lithium metaborate/tetraborate fusion and nitric acid digestion at the ACTLABS Activation Laboratories Ltd. (Ancaster, Canada).

4 Results

4.1 Petrography and mineralogy

4.1.1 Alkaline magmatic rocks and carbonatites

The primary lithologies under study, consist of Oligocene (~25 Ma) alkaline igneous and carbonatitic rocks, as well as Miocene alkaline lithologies (K–Ar age of 20.6±1.7 Ma; Le Bas et al., 1986), that form part of the FBC. Their outcrops extend across kilometer-scale areas but exhibit high heterogeneity at a detailed level due to the occurrence of numerous small intrusions, ranging in size from metric to decimetric dimensions (Figs. 2a, b).

At a mineralogical level, separation of the different types of alkaline rocks found in the FBC is complex because these lithologies are intimately associated and infiltrate diffusely, leading to the formation of hybrid intrusions. The materials with the most mafic composition correspond to pyroxenites and melteigites, and their formation is associated with the earliest magmatic fractions. However, these are commonly spatially associated with more differentiated rocks, mainly ijolites, nepheline syenites, and syenites. All these lithologies have a relatively simple mineralogy, characterized by varying proportions of nepheline (10-30% modal) and potassium feldspar (50-80% modal), associated with aegirine-augite and biotite (10-30%

modal). A set of accessory minerals with varying proportions (always less than 5% modal) also occur, including ilmenite, titanite, zircon, and fluorapatite.

At a textural level, the alkaline series lithologies of the FBC present granular textures with millimeter-sized euhedral grains. However, in some of the intrusions in sectors 2 and 3, pegmatitic syenites-ijolites were detected with centimeter-sized grains characterized by the presence of large aegirine-augite crystals.

Some of the intrusions described in the three sectors show aphanitic textures caused by faster cooling, resulting in rocks with similar mineralogy but extrusive-type textural characteristics. Therefore, due to their textural features, some dikes and apophyses, although mineralogically equivalent, should be classified as trachytes and phonolites.

Carbonatitic intrusions commonly co-occur with the alkaline rocks, sharing similar morphology, textures, and spatial distribution within the outcrops (Figure 2e). Furthermore, alkaline and/or carbonatitic intrusions can be occasionally associated with mafic intrusions, primarily pyroxenites and alkaline gabbros. In addition, a subsequent set of mafic dikes with basaltic composition overlaps the previous intrusive bodies (Figs. 2a, b).

All carbonatites described in different outcrops from sectors 1 and 3 are predominantly composed of calcite (95% modal) and can thus be classified as calciocarbonatites (Le Maitre, 2005). None of the studied samples shows the occurrence of ferromagnesian carbonates such as ankerite, dolomite, and/or siderite, as well as REE carbonates. Texturally, calcite occurs as euhedral crystals ranging in size from millimetres to centimetres, often recrystallized and exhibiting polysynthetic twinning. In some cases, a secondary micritic calcite matrix is present, filling interstitial spaces and fractures.

The major element composition of calcite is relatively consistent across all the carbonatite samples. Notably, there are significant contents of SrO, with values of up to 5.43 wt%, while REEs are absent from the carbonate composition (Table S2).

The accessory mineralogy (~5% modal) comprises disseminated phases within the calcium carbonate. Among them, the occurrence of minerals from the spinel group, including magnetite (Figure 3a), and primarily jacobsite, occurring as subhedral crystals of up to 50 μm (Figure 3b). Another characteristic mineral is perovskite, occurring as subhedral crystals of up to 100 μm. These grains are remarkable for their significant Nb contents, as described in other carbonatitic localities worldwide (Torró et al., 2012). Britholite also occurs as subhedral crystals of up to 100 μm (Figure 3b). This primary britholite contains significant LREE content (Figure 4), and its alteration leads to the formation of secondary REE-enriched

phosphates, mainly monazite-Nd (Figure 3c), which also contains substantial amounts of La and Ce (Figure 4). REEs, in addition to occurring in primary britholite and secondary monazite, were also detected in tiny pyrochlore grains, heterogeneously disseminated in the calcite groundmass (Figure 3b). In some cases, pyrochlore forms euhedral crystals of up to 20 μm, also included in calcite (Figure 3d). This pyrochlore shows slight zoning towards plumbopyrochlore (Christy and Atencio, 2013), with significant enrichment in Pb observed at grain borders (Figure 3d).

Carbonatites can be affected by certain contact metamorphism, especially in sectors 1 and 3 (Figure 1) and may exhibit a slightly different mineralogy from the one described thus far. This is characterized by the occurrence of skarn-type metamorphic minerals, formed due to the interaction between carbonatites and spatially associated silica-rich rocks. Among these minerals, there are subhedral crystals of andradite, up to 30 μm in size, implanted in a matrix of secondary calcite and phlogopite, exhibiting pronounced zoning with kerimasite cores (Figure 3e). In these areas, the occurrence of REE mineralizations associated with allanite (Figure 3f) is also typical. Allanite occurs as granular aggregates associated with hydrothermal secondary sulfates, primarily baryte (Figure 3f), but occasionally celestine (Figure 3c).

This particular mineralogy, typically associated with skarn formations, emerges from the interaction between a carbonatite intrusion and surrounding silicate rocks, in contrast to the typical process. It has recently gained attention from several researchers in various carbonatite locations worldwide, who have coined the term antiskarn to describe it (Anenburg and Mavrogenes, 2018; Yaxley et al., 2022).

4.1.2 Weathering products

In certain areas within the three studied sectors (Figure 1), there is evidence of the development of characteristic shallow geological formations consistently associated with weathering, which affect the outlined magmatic lithologies (Figs. 5, 6). These geological products were studied through the analysis of six alteration profiles, developed on carbonatites (Agua Salada and Aulagar) and syenites (Palomares ravine, FV-30 road, Las Peñitas quarry, and Pájara) (Figure 1).

The carbonatite-calcrete sections generally consist of centimetre-scale calcrete veins injected into the bedrock, seemingly without any apparent connection to the current upward lithosol (Figure 5). In general, the development of soils or weathering products was not detected on carbonatites in any of the studied sectors of the FBC.

Weathering products developed on syenite bedrock are generally more abundant, and the corresponding alteration profiles are better preserved than in carbonatites. The cambic B horizon displays reddish to yellowish colorations (5YR6/6), with a thickness of up to 20-30 cm. Additionally, it is common to find BC horizons instead of B horizons, while the C horizon is well-developed, reaching a 30-40 cm thickness at certain levels of the profile (Figure 6). Furthermore, except for the Las Peñitas profile (E profile, Figure 1), centimetre-scale calcrete bands (Bk; Jahn et al., 2006) were also detected in deeper layers across all the studied profiles.

In terms of mineralogical composition, carbonatite profiles exhibit significant changes due to weathering. In general, weathering processes lead to a reduction in calcite, the disappearance of fluorapatite, and the formation of secondary minerals like palygorskite (Figure 7). The contribution from lateral slope movement is also evident through the presence of residual plagioclase and clinopyroxene.

In the case of syenite weathering profiles, illite/chlorite and kaolinite are the predominant secondary products, followed by muscovite and palygorskite (Figure 7). Other minerals such as quartz were also detected, even in the C horizons.

4.2 Bulk-rock and mineral geochemistry

Chemical analysis of the major, minor and trace elements were carried out in order to evaluate the geochemical features and the distribution of REEs, on 25 representative samples of igneous rocks from the FBC, including trachytes, phonolites, syenites, ijolites and carbonatites (Table S3). In addition, we also analysed 21 samples of weathering products (Table S4).

The total REY (REEs plus yttrium) content in the FBC igneous rocks exhibits widespread and significant enrichment in comparison to the average crustal values (~125 ppm, Rudnick and Gao, 2014). Notably, the extrusive and magmatic alkaline lithologies (trachytes and phonolites as well as syenites and ijolites) show variable REY values ranging between about 230 and 1,400 ppm (Table S3). In contrast, the carbonatitic rocks exhibit REY content more than ten times greater than the alkaline lithologies, with specific samples reaching maximum values of up to about 10,300 ppm, as evidenced in sample 85a sourced from a carbonatite outcrop in sector 1 (Table S3).

The weathered magmatic rocks, though moderately significant in REY content relative to the average crustal values (Table S4), still exhibit slightly lower levels compared to the content observed in the associated alkaline and carbonatitic protoliths (Table S3). A contrasting pattern emerges in the calcretes,

where REY values experience a sharp reduction, presenting virtually negligible values ranging between 20 and 72 ppm REY. These levels are significantly below the average Earth's crust values (Rudnick and Gao, 2014) and are markedly lower than those observed in both the alkaline lithologies and, particularly, the carbonatites of the FBC.

REE normalized diagrams further underscore this distribution, portraying elevated content in the carbonatites, followed by the alkaline rocks (Figure 8a). Meanwhile, the weathered magmatic rocks and calcretes (Figure 8b) display significantly lower values. All studied lithologies exhibit clear negative patterns, indicative of enrichment in LREEs relative to HREEs. Notably, carbonatites and alkaline rocks (Figure 8a) exhibit a flattening of these negative patterns in the final segment, indicating a certain degree of HREE enrichment.

The FCB carbonatites exhibit a depletion in some critical elements commonly associated with this lithology such as Nb or Ta (Table S3). Negative anomalies of both Nb and Ta are clearly observed in the multi-element diagrams of carbonatite samples (Figure 9a). However, given the presence of pyrochlore in the carbonatites, these anomalies in Nb and Ta are likely not indicative. We interpret that the low concentrations of these elements could be attributed to an analytical artifact that would underestimate the contents of High Field Strength Elements (HFSE) due to the challenge of pyrochlore dissolution in the analytical digestion protocols employed. These protocols have been primarily devised to assess the contents of REEs rather than HFSE. Additionally, alkaline rock patterns also show a distinctive negative anomaly in Sr (Figure 9b). As for the weathering products, their contents of other minor elements do not indicate significant concentrations of metals or critical elements like Nb or Ta (Table S4). The multi-element diagrams for the calcretes exhibit a negative Ta anomaly (Figure 9c), while the patterns of weathered magmatic rocks do not reveal notable anomalies in any group of elements (Figure 9d).

A specific geochemical study of REE distribution in the six studied weathering profiles was also conducted (Figure 10). The main objective was to evaluate the geochemical interactions between the protolith and the related weathering lithologies, with the aim of detecting potential REE enrichments or depletions caused by weathering processes.

In the exchange patterns of calcretes spatially associated with carbonatitic protoliths, as analyzed in the Agua Salada and Aulagar ravine profiles (Figs. 10A, B), REE concentrations are two orders of magnitude lower than in the carbonatite (Figure 10A), as also previously determined from the REE diagrams (Figure 8). Notably, it was found that the REE concentration is directly proportional to the distance from the

protolith (Figure 10B), and calcrete samples with the highest REE concentrations (sample 14; Figure 10) were found in closer proximity to the primary carbonatites than more REE depleted samples (samples 15 and 18; Figure 10B). In addition, although the values of all elements are depleted in the calcrete patterns, there is a greater depression in LREE than in HREE relative to the protolith, resulting in typically positive patterns, except for sample 76 from the Agua Salada ravine, where a clear inverse trend is observed (Figure 10A).

In general, the diagrams in Figure 10 show that weathering products on syenites exhibit enrichment relative to the protolith (green areas in Figs. 10C, D, E). However, calcrete samples, whether derived from carbonatites or syenites, consistently show depletions compared to the protolith contents (reddish areas in Figs. 10C, D, F). The diagrams corresponding to the weathering products generated on syenites exhibit similar morphologies (Figs. 10C, D, E, F). Overall, these lithologies are characterized by enrichment in REEs relative to the protolith as well as V-shaped patterns, featured by the presence of a negative anomaly in Eu, which is also reported in all C and B horizons developed on syenites, except sample 61 (Figure 10C), and is likely related to plagioclase crystallization.

5 Discussion

5.1 REE distribution on the FBC magmatic rocks

The FBC magmatic rocks, in the three study sectors, encompass alkaline lithologies (trachytes, phonolites, syenites, melteigites, and ijolites) as well as carbonatites. Regarding the group of alkaline rocks, the detected REE content varies between 214 and 1,330 ppm (Table S3), significantly higher than the average concentration determined in the Earth's crust (~125 ppm, Rudnick and Gao, 2014). However, this finding is not surprising, and the observed values in Fuerteventura are not anomalous, as these types of lithologies typically exhibit REE concentrations within this range (Dostal, 2017). Therefore, the measured REE concentrations are neither significant nor sufficiently elevated to hypothetically consider these lithologies as a potential non-conventional deposit of these critical elements in the FBC.

On the other hand, FBC carbonatites present significantly higher values in terms of REE content. In the studied carbonatite samples from sectors 1 and 3 (carbonatites do not outcrop in sector 2), REE content ranges between about 1300 ppm and 10,300 ppm. The latter value corresponds to the richest REE-detected sample in the entire FBC, which is located in the Agua Salada ravine area of sector 1 (Table S3; Figure 1).

The reported REE content values in the FBC carbonatites are similar to the general average concentrations found in other locations worldwide where carbonatites are exploited for REE extraction. This is the case, for example, of Bayan Obo, the largest REE deposit in the world (Lai et al., 2015; Liu et al., 2018). In this locality, high-grade carbonatites exhibit average concentrations of 2880 ppm (Wu et al., 2008; Smith et al., 2015, 2016), which are equivalent to those measured in some of the samples from Fuerteventura. It should be noted that low-grade carbonatite ore from Bayan Obo presents extremely high values in comparison to the FBC, with REE concentrations reaching 30,750 ppm (Chao et al., 1997; Smith et al., 2016).

Another significant example is the Mountain Pass carbonatite in California, USA (Olson et al., 1954; Haxel, 2005). In this REE deposit, average value across the whole complex are around 2580 ppm (Castor et al., 2008; Mariano and Mariano, 2012; Smith et al., 2016), also in line with REE concentrations detected in the present study for the FBC carbonatites.

This comparative analysis can also be carried out using normalized REE values (Figure 11). In this regard, FBC carbonatites are significantly depleted in LREE compared to those from Bayan Obo (Yang et al., 2019) and Mountain Pass (Castor et al., 2008), although they show similar values to other REE deposits associated with carbonatites, such as those in Ashram, Canada (Beland and Jones, 2021) and Bear Lodge, USA (Moore et al., 2015; Smith et al., 2016; Figure 11). However, the pattern of the Fuerteventura carbonatites exhibits a slightly less pronounced slope, indicating a higher relative content of HREE, which are considered the materials with the highest risk of supply among all the CRMs defined by the EC (European Commission, 2023a). In fact, in the FBC carbonatites, the normalized HREE values are equivalent to those reported in the primary carbonatitic rocks from the deposits of Bayan Obo (China) and Mountain Pass (USA) (Figure 11). The relative significant HREE content reported in FBC carbonatites holds particular significance. The use of HREEs, such as Yb, Er, and Tm, is of particular interest in cutting-edge photonic and nanotechnology applications.

At the mineralogical level, it was observed that, in the FBC carbonatites, the main REE-hosting minerals are accessory phases; primarily minerals from the pyrochlore group, found as disseminated euhedral micro-crystals implanted in primary calcite (Figs. 3b, d). Another REE-bearing mineral in the FBC carbonatites is britholite, which exhibits significant LREE content. However, this mineral is commonly altered to monazite (Figs. 3c, 4), interpreted as a secondary phase but also a carrier of these critical elements (Chen et al., 2017).

Another noteworthy aspect is the lack of REE fluorcarbonates like bastnäsite $REE(CO_3)F$, parisite $Ca(REE)_2(CO_3)_3F_2$, synchysite $Ca(REE)(CO_3)_2F$ or huanghoite $Ba(REE)(CO_3)_2F$. They do not occur in the FBC, as they do in other REE deposits associated with, for example, the Bayan Obo carbonatite or the Sulphide Queen carbonatite from Mountain Pass (Castor et al., 2008; Smith et al., 2015, 2016).

5.2 REE distribution on the associated weathering products

The weathering materials developed on magmatic rocks, also analysed for their REE concentrations, constitute the remnants of soils that were interpreted as developed under wetter conditions during a humid phase of the oxygen isotope stage 2, spanning from 29 to 20 thousand years BP (Huerta et al., 2016). This period aligns with the last glacial maximum, marked by heightened humidity in the Canary Islands, resulting in slope erosion and the formation of talus flatiron (Gutiérrez-Elorza et al., 2013). Over time, these materials have undergone substantial volume reduction due to human-driven deforestation and erosion, primarily before the 15th century (Machado-Yanes, 1996). Notably, topography plays an essential role in the distribution of these weathering profiles and influences specific physical attributes such as slope (FAO/UNESCO, 1974).

The studied weathering products developed on syenite rocks (profiles C, D, E, F; Figs. 1, 7) are classified by FAO/UNESCO (1974) as eutric cambisols, reflecting a Mediterranean climate condition. Indeed, on the African continent, which is adjacent to the Canary Islands, eutric cambisols are primarily found within the tropical subhumid zone, gradually transitioning into the semi-arid zone (FAO/UNESCO, 1974). These syenite weathering profiles exhibit better-preserved characteristics and a more significant extent compared to those studied in carbonatites (profiles A and B; Figs. 1, 7). In general, intensive weathering plays a crucial role in the formation of REE deposits, as these elements tend to be concentrated in such geological formations compared to others leached during the weathering process. This phenomenon is exemplified in several locations worldwide, where REE deposits associated with weathering products occur: for instance, Bear Lodge in the USA (Andersen et al., 2017), Chuktukon and Tomtor in Russia (Kravchenko and Pokrovsky, 1995; Kravchenko et al., 2003; Chebotarev et al., 2017), Las Mercedes in the Dominican Republic (Torró et al., 2017), Araxá in Brazil (Braga and Biondi, 2023), and Mount Weld in Australia (Zhukova et al., 2021; Chandler et al., 2024), among many others. However, the weathering processes on Fuerteventura are characterized by fluctuating climatic conditions and intense erosion in the context of a typical Mediterranean climate, which is in turn characterized by drier conditions and a lower propensity for

intense weathering compared to tropical climates. The weathering processes on Fuerteventura do not therefore typically lead to the development of laterites and mature weathering profiles, since these conditions do not favor the formation and subsequent preservation of these products, particularly within the carbonatite bedrock areas.

5.3 Fuerteventura carbonatites as potential REE source

Based on the mineralogical and geochemical data, it can be concluded that, among the lithologies studied in the FBC, only the carbonatites are favorable targets for REEs exploration. Therefore, the primary alkaline rocks, as well as the entire suite of corresponding secondary weathering products, can be ruled out.

The geochemical data obtained from the oceanic carbonatites of Fuerteventura, exemplified in multielement and REE diagrams (Figure 8), suggest a petrogenetic affinity with carbonatites associated with intracontinental rift geological settings. This similarity has also been previously highlighted by other authors such as Carnevale et al. (2021) who, based on stable isotope data ($\delta^{13}C$ and $\delta^{18}C$) and noble gases isotopic composition (He, Ne, Ar), suggested that oceanic and continental carbonatites were comparable in petrogenetic terms. Therefore, despite the lingering questions about the formation processes of oceanic carbonatites, their assessment as a possible source of critical metals, especially REEs, could be considered in the same way as their continental counterparts.

However, when considering a more detailed assessment of the sectors where the FBC carbonatites outcrop, it is essential to note that the distribution of these outcrops and thus potential REE mineralization is not straightforward. The carbonatite outcrops have a very limited surface distribution, in the order of metres (Figure 2e), and exhibit complex structural features influenced by shear metamorphism (Figure 2c) and overlapping episodes of intrusive activity that resulted in swarms of dikes with intricate distributions (Figs. 2a, b). Hence, these general features of the carbonatite outcrops make it imperative to validly estimate their volume and to carry out more precise studies of their depth distribution.

Then, it is important to highlight that any attempt to assess potential REE deposits linked to FBC carbonatites must consider the irregular distribution of these mineralizations. In addition, it should also be considered the existence of regulatory constraints that may stem from the allocation of land for strategic military activities, as well as environmental considerations to safeguard natural and marine-coastal areas, especially bearing in mind that Fuerteventura is a UNESCO biosphere reserve territory. This latter point is particularly pertinent for a specific area within sector 3 (Figure 1). Therefore, any comprehensive analysis

of the potential of FBC carbonatites as REE sources must also factor in these potential restrictions tied to land use regulations aimed at upholding the broader socio-economic, environmental, and societal interests inherent to a distinctive site like the island of Fuerteventura.

6 Conclusions

A preliminary study of the distribution of REEs was conducted through mineralogical and geochemical analyses of alkaline and carbonatitic igneous rocks within the FBC, along with associated weathering products. Based on the gathered data and their corresponding interpretations, our findings can be summarized as follows:

(i) The concentrations of REEs present in the alkaline and carbonatitic rocks of the FBC are significant and exceed the average values attributed to the Earth's crust.

(ii) The weathering products developed on these magmatic rocks do not exhibit significant REE enrichment.

(iii) Calcified horizons (Bk, calcretes), spatially related with carbonatites, have practically negligible concentrations of REE elements. Colluvial processes may have influenced the lateral transport and accumulation of REEs in Pleistocene-Holocene deposits distant from the source area.

(iv) The detected concentrations of REY in carbonatites range up to about 10,300 ppm, which is a comparable concentration to other locations hosting significant deposits of these critical elements worldwide.

(v) Within carbonatites, REEs are primarily hosted in two accessory mineral phases: (1) oxides belonging to the pyrochlore group; and (2) phosphates. In this second group, primary phases such as REE-bearing britholite can be distinguished, as well as monazite generated as a secondary product from the britholite alteration.

(vi) Primary calcite in the Fuerteventura carbonatites is not the predominant host of REEs. It displays a highly homogeneous composition with insignificant Fe-Mg content and negligible REEs.

(vii) The complex structural features of the studied FBC outcrops (deformation, metamorphism, swarms of dikes from different intrusive pulses...) make it essential to conduct more detailed studies to quantify real REE resources.

(viii) All the studied sectors contain outcrops located in restricted areas due to environmental or military use concerns. Any further detailed analysis of REE distribution in the FBC carbonatites must take into account the environmental, socio-economic, and geostrategic factors.

Acknowledgements

This research was funded by the "Tierras Raras" project (SD-22/25) and the "MAGEC-REEmounts" project (ProID-20211010027) of the Canarian Agency for Research, Innovation and Information Society (ACIISI by its initials in Spanish) of the Canary Islands Government. Funding support was also provided by the project "Materials for Advanced Energy Generation" (ENE2013-47826-C4-4-R), "3D Printed Advanced Materials for Energy Applications" (ENE2016-74889-C4-2-R) and "Estudio de los procesos magmáticos, tectónicos y sedimentarios involucrados en el crecimiento temprano de edificios volcánicos oceánicos en ambiente de intraplaca" (CGL2016-75062-P), all funded by the Government of Spain. The collection of samples in specific protected areas required authorization from the Fuerteventura Island Government. We appreciate the cooperation and assistance provided by the Spanish Army, especially by the soldier Liberto Yeray Puga Acosta, who facilitated our access to the Pájara CMT restricted military area to carry out sampling. We thank Gerard Lucena from the LPGiP-MCNB for his thorough work in the elaboration of polished thin sections. We would also like to express our acknowledgements to professor Michael Anenburg, an anonymous reviewer, and editor Johan Lissenberg for their constructive and enriching comments and corrections, which greatly improved the initial version of this manuscript

Statements and Declarations

Data availability statement

The authors confirm that the data supporting the findings of this study are available within the article and its supplementary materials.

Competing interests

The authors declare no competing interests. The funders had no role in the design of the study, in the collection of samples, the analyses, the interpretation of data, the writing of the manuscript nor the decision to publish these results.

Author contributions

Conceptualization: MC, IM, LQ, JY, JM; fieldwork and sampling: MC, IM, LQ, JY, RC, AA, JM; methodology: MC, IM, JY, JM; validation of results: MC, IM, LQ, JY, RC, JMR, JM; data curation: MC, IM, JM; writing-original draft preparation: MC, IM, JY, JM; writing-review editing: MC, IM, LQ, JY, RC, JMR, JM; supervision: IM, JY, JM; project administration: JMR, JM; funding acquisition: IM, JY, RC, JMR, JM.

Additional information

Supplementary tables are available in the online version at https: XXXXX

References

Acosta-Mora, P., Domen, K., Hisatomi, T., Lyu, H., Méndez-Ramos, J., Ruiz-Morales, J. C., Khaidukov, N. M.: "A bridge over troubled gaps": up-conversion driven photocatalysis for hydrogen generation and pollutant degradation by near-infrared excitation, Chem. Commun, 54, 1905 –1908 https://doi.org/10.1039/C7CC09774C, 2018.

Aiglsperger, T., Proenza, J. A., Lewis, J. F., Labrador, M., Svojtka, M., Rojas-Purón, A., Longo, F., Ďurišová, J.: Critical metals (REE, Sc, PGE) in Ni laterites from Cuba and the Dominican Republic, Ore Geol. Rev., 73, 127–147, https://doi.org/10.1016/j.oregeorev.2015.10.010, 2016.

Ahijado, A.: Las intrusiones plutónicas e hipoabisales del sector meridional del Complejo Basal de Fuerteventura, Doctoral Thesis, Universidad Complutense de Madrid, 392 p., 1999.

Ahijado, A., Casillas, R., Nagy, G., Fernández, C.: Sr-rich minerals in a carbonatite skarn, Fuerteventura, Canary Islands (Spain), Mineralogy and Petrology, 84, 107–127, https://doi.org/10.1007/s00710-005-0074-8, 2005.

Alonso, E., Sherman, A. M., Wallington, T. J., Everson, M. P., Field, F. R., Roth, R., Kirchain, R. E.: Evaluating Rare Earth Element Availability: A Case with Revolutionary Demand from Clean Technologies, Environ. Sci. Technol., 46, 3406–3414, https://doi.org/10.1021/es203518d, 2012.

Alonso-Zarza, A. M., Silva, P. G.: Quaternary laminar calcretes with bee nests evidences of small-scale climatic fluctuations, Eastern Canary Islands, Spain, Palaeogeogr. Palaeoclimatol. Palaeoecol., 178, 119–135, https://doi.org/10.1016/S0031-0182(01)00405-9, 2002.

Alonso-Zarza, A. M., Rodríguez-Berriguete, Á., Casado, A. I., Martín-Pérez, A., Martín-García, R., Menéndez, I., Mangas, J.: Unravelling calcrete environmental controls in volcanic islands, Gran Canaria Island, Spain, Palaeogeogr. Palaeoclimatol. Palaeoecol., 554, 109797, https://doi.org/10.1016/j.palaeo.2020.109797, 2020.

Ancochea, E., Brändle, J. L., Cubas, C. R., Hernán, F., Huertas, M. J.: Volcanic complexes in the eastern ridge of the Canary Islands: the Miocene activity of the Island of Fuerteventura, Journal of Volcanology and Geothermal Research, 70, 183–204, https://doi.org/10.1016/0377-0273(95)00051-8, 1996.

Ancochea, E., Barrera, J. L., Bellido, F.: Canarias y el vulcanismo neógeno peninsular. Geología de España, 635-682. In: Aparicio, A., Hernán, F., Cubas, C. R., Araña, V., 2003, Fuentes mantélicas y evolución del volcanismo canario, Estudios Geológicos, 59, 5–13, https://doi.org/10.3989/egeol.03591-477, 2004.

Andersen, A. K., Clark, J. G., Larson, P. B., Donovan, J. J.: REE fractionation, mineral speciation, and supergene enrichment of the Bear Lodge carbonatites, Wyoming, USA, Ore Geology Reviews, 89, 780–807, https://doi.org/10.1016/j. oregeorev.2017.06.025, 2017.

Anenburg, M., Mavrogenes, J.A., Carbonatitic versus hydrothermal origin for fluorapatite REE-Th deposits: experimental study of REE transport and crustal "antiskarn" metasomatism, American Journal of Science, 318, 335–366, https://doi.org/10.2475/03.2018.03, 2018.

Anenburg, M., Broom-Fendley, S., Chen, W.: Formation of Rare Earth Deposits in Carbonatites, Elements, 17, 327–332, https://doi.org/10.2138/gselements.17.5.327, 2021.

589 Balcells, R., Barrera, J. L., Gómez, J. A., Cueto, L. A., Ancochea, E., Huertas, M. J., Ibarrola, E., Snelling,
590 N.: Edades radiométricas en la Serie Miocena de Fuerteventura (Islas Canarias), Bol. Geol. Min., 35,
591 450–470, 1994.
592 Balaram, V.: Rare earth elements: A review of applications, occurrence, exploration, analysis, recycling,
593 and environmental impact, Geoscience Frontiers, 10, 1285–1303,
594 https://doi.org/10.1016/j.gsf.2018.12.005, 2019.
595 Balogh, K., Ahijado, A., Casillas, R., Fernández, C.: Contributions to the chronology of the Basal Complex
596 of Fuerteventura, Canary Islands, Journal of Volcanology and Geothermal Research, 90, 81–101,
597 https://doi.org/10.1016/S0377-0273(99)00008-6, 1999.
598 Bao, Z., Zhao, Z.: Geochemistry of mineralization with exchangeable REY in the weathering crusts of
599 granitic rocks in South China, Ore Geol. Rev., 33, 519–535,
600 https://doi.org/10.1016/j.oregeorev.2007.03.005, 2008.
601 Barrera, J. L., Fernández-Santín, S., Fúster, J. M., Ibarrola, E.: Ijolitas-Sienitas-Carbonatitas de los Macizos
602 del Norte de Fuerteventura, Bol. Geol. Min., TXCII-IV, 309–321. ISSN 0366-0176, 1993.
603 Barteková, E., Kemp, R., National strategies for securing a stable supply of rare earths in different world
604 regions, Resources Policy, 49, 153–164, https://doi.org/10.1016/j.resourpol.2016.05.003, 2016.
605 Beland, C. M. J., William-Jones, A. E.: The mineralogical distribution of the REE in carbonatites: A
606 quantitative evaluation, Chemical Geology, 585, 120558,
607 https://doi.org/10.1016/j.chemgeo.2021.120558, 2021.
608 Berger, A., Janots, E., Gnos, E., Frei, R., Bernier, F., Rare earth element mineralogy and geochemistry in
609 a laterite profile from Madagascar. Applied Geochemistry 41, 218–228,
610 https://doi.org/10.1016/j.apgeochem.2013.12.013, 2014.
611 Borst, A. M., Smith, M. P., Finch, A. A., Estrade, G., Villanova-de-Benavent, C., Nason, P., Marquis, E.,
612 Horsburgh, N. J., Goodenough, K. M., Xu, C., Kynický, J., Geraki, K.: Adsorption of rare earth
613 elements in regolith-hosted clay deposits, Nat. Commun., 11, 4386, https://doi.org/10.1038/s41467-
614 020-17801-5, 2020.
615 Braga, J. M., Biondi, J. C.: Geology, geochemistry, and mineralogy of saprolite and regolith ores with Nb,
616 P, Ba, REEs (+ Fe) in mineral deposits from the Araxá alkali-carbonatitic complex, Minas Gerais
617 state, Brazil, Journal of South American Earth Sciences, 125, 104311,
618 https://doi.org/10.1016/j.jsames.2023.104311, 2023.
619 Braun, J. J., Pagel, M., Herbilln, A., Rosin, C.: Mobilization and redistribution of REEs and thorium in a
620 syenitic lateritic profile: A mass balance study, Geochem. Cosmochim. Acta, 57, 4419–4434.
621 https://doi.org/10.1016/0016-7037(93)90492-F, 1993.
622 Carnevale, G., Caracausi, A., Correale, A., Italiano, L., Rotolo, S.G., An Overview of the Geochemical
623 Characteristics of Oceanic Carbonatites: New Insights from Fuerteventura Carbonatites (Canary
624 Islands), Minerals, 11, 203. https://doi.org/10.3390/min11020203, 2021.
625 Casillas, R., Nagy, G., Demény, A., Ahijado, A., Fernández, C.: Cuspidine–niocalite–baghdadite solid
626 solutions in the metacarbonatites of the Basal Complex of Fuerteventura (Canary Islands). Lithos
627 105:25–41. https://doi.org/10.1016/j.lithos.2008.02.003, 2008.

Casillas, R., Démeny, A., Nagy, G., Ahijado, A., Fernández, C.: Metacarbonatites in the Basal Complex of Fuerteventura (Canary Islands). The role of fluid/rock interactions during contact metamorphism and anatexis, Lithos, 125, 503–520, https://doi.org/10.1016/j.lithos.2011.03.007, 2011.

Castor, S. B.: The Mountain Pass rare-earth carbonatite and associated ultrapotassic rocks, California, The Canadian Mineralogist, 46, 779–806, https://doi.org/10.3749/canmin.46.4.779, 2008.

Chakhmouradian, A. R., Wall, F.: Rare Earth Elements: Minerals, Mines, Magnets (and More), Elements, 8, 333–340, https://doi.org/10.2113/gselements.8.5.333, 2012.

Chao, E. C. T., Back, J. M., Minkin, J. A., Tatsumoto, M., Wang, J., Conrad, J. E, McKee, E. H., Hou, Z. L., Meng, Q. R., Huang, S. G.: The sedimentary carbonate-hosted giant Bayan Obo REE-Fe-Nb ore deposit of Inner Mongolia, China: a corner stone example for giant polymetallic ore deposits of hydrothermal origin, USGS Bulletin, 2143, 65, https://doi.org/10.3133/b2143, 1997.

Chandler, R., Bhat, G., Mavrogenes, J., Knell, B., David, R., Leggo, T.: The primary geology of the Paleoproterozoic Mt Weld carbonatite complex, Western Australia, Journal of Petrology, 65, 2, https://doi.org/10.1093/petrology/egae007, 2024.

Chebotarev, D. A., Doroshkevich, A., Klemd, R., Karmanov, N.: Evolution of Nb- mineralization in the Chuktukon carbonatite massif, Chadobets upland (Krasnoyarsk Territory, Russia), Periodico di Mineralogia, 86, 99–118, https://doi.org/10.2451/2017PM733, 2017.

Chen, W., Honghui, H., Bai, T., Jiang, S.: Geochemistry of Monazite within Carbonatite Related REE Deposits, Resources, 6, 51, https://doi.org/10.3390/resources6040051, 2017.

Chiquet, A., Michard, A., Nahon, D., Hamelin, B.: Atmospheric input vs in situ weathering in the genesis of calcretes: an Sr isotope study at Gálvez (Central Spain), Geochim. Cosmochim. Acta, 63, 311–323, https://doi.org/10.1016/S0016-7037(98)00271-3, 1999.

Christy, A. G., Atencio, D.: Clarification of status of species in the pyrochlore supergroup, Mineralogical Magazine, 77, 13–20, https://doi.org/10.1180/minmag.2013.077.1.02, 2013.

Christy, A.G., Pekov, I.V., Krivovichev, S.G., The Distinctive Mineralogy of Carbonatites, Elements, 17, 333–338, https://doi.org/10.2138/gselements.17.5.333, 2021.

Coello, J., Cantagrel, J. M., Hernán, F., Fúster, J. M., Ibarrola, E., Ancochea, E., Casquet, C., Jamond, C., Díaz-de-Terán, J. R., Cendrero, A.: Evolution of the Eastern volcanic ridge of Canary Islands based on new K-Ar data, Journal of Volcanology and Geothermal Research, 53, 251–274, https://doi.org/10.1016/0377-0273(92)90085-R, 1992.

Connelly, N. G., Hartshorn, R. M., Damhus, T., Hutton, A. T.: Nomenclature of Inorganic Chemistry IUPAC Recommendations 2005, RSC Publishing, Cambridge, ISBN-0-85404-438-8, 2005.

Courtillot, V., Davaille, A., Besse, J., Stock, J.: Three distinct types of hotspots in the Earth's mantle, Earth Planet. Sci. Letters, 205, 295–308, https://doi.org/10.1016/S0012-821X(02)01048-8, 2003.

De Ignacio, C., Muñoz, M., Sagredo, J., Carbonatites and associated nephelinites from São Vicente, Cape Verde Islands, Min., Mag., 76, 311–355, doi:10.1180/minmag.2012.076.2.05, 2012.

Demény, A., Ahijado, A., Casillas, R., Vennemann, T.W., Crustal contamination and fluid/rock interaction in the carbonatites of Fuerteventura (Canary Islands, Spain): A C, O, H isotope study, Lithos, 44, 101–115, https://doi.org/10.1016/S0024-4937(98)00050-4, 1998.

Dostal, J.: Rare Earth Element Deposits of Alkaline Igneous Rocks, Resources, 6, 34–46, https://doi.org/10.3390/resources6030034, 2017.

Doucelance, R., Hammouda, T., Moreira, M., Martins, J.C., Geochemical constraints on depth of origin of oceanic carbonatites: The Cape Verde case, Geochim. Cosmochim. Acta, 74, 7261–7282, https://doi.org/10.1016/j.gca.2010.09.024, 2010.

Doucelance, R., Bellot, N., Boyet, M., Hammouda, T., Bosq, C., What coupled cerium and neodymium isotopes tell us about the deep source of oceanic carbonatites, Earth Planet. Sci. Lett., 407, 175–186, https://doi.org/10.1016/j.epsl.2014.09.042, 2014.

European Commission: European Green Deal, https://commission.europa.eu/strategy-and-policy/priorities-2019-2024/european-green-deal_en, 2019.

European Commission: Study on the Critical Raw Materials for the EU 2023 – Final Report, https://op.europa.eu/en/publication-detail/-/publication/57318397-fdd4-11ed-a05c-01aa75ed71a1 - https://doi.org/10.32873/725585, 2023a.

European Commission, Regulation of the European Parliament and of the Council establishing a framework for ensuring a secure and sustainable supply of critical raw materials and amending Regulations (EU) 168/2013, (EU) 2018/858, 2018/1724 and (EU) 2019/1020, https://eur-lex.europa.eu/legal-content/EN/TXT/?uri=CELEX%3A52023PC0160, 2023b.

FAO/UNESCO: Soil Map of the World Project 1:5000000, Chart VI1, https://www.fao.org/soils-portal/data-hub/soil-maps-and-databases/faounesco-soil-map-of-the-world/en/, 1974.

Feraud, G., Giannerini, G., Campredon, R., Stillman, C.J.: Geochronology of some canarian dike swarms: contribution to the volcano-tectonic evolution of the archipielago, J. Volcanol. Geotherm. Res., 25, 29–52, https://doi.org/10.1016/0377-0273(85)90003-4, 1985.

Fernández, C., Casillas, R., Ahijado, A., Perelló, V., Hernández-Pacheco, A.: Shear zones as a result of intraplate tectonics in oceanic crust: the example of the Basal Complex of Fuerteventura (Canary Islands), Jour. Struct. Geol., 19, 41–57, https://doi.org/10.1016/S0191-8141(96)00074-0, 1997.

Frisch, T.: In: Schmincke, H. U., Sumita, M.: Geological evolution of the Canary Islands: a young volcanic archipelago adjacent to the old African continent, Bull Volcanol., 74, 1255–1256, https://doi.org/10.1007/s00445-012-0605-1, 2012.

Fúster, J. M., Cendrero, A., Gastesi, P., Ibarrola, E., López-Ruiz, J.: Geología y volcanología de las Islas Canarias- Fuerteventura, Instituto “Lucas Mallada”, Consejo Superior de Investigaciones Científicas, Madrid. 239 pp, 1968.

Goodenough, K. M., Schilling, J., Jonsson, E., Kalvig, P., Charles, N., Tuduri, J., Deady, E. A., Sadeghi, M., Schiellerup, H., Müller, A., Bertrand, G., Arvanitidis, N., Eliopoulos, D. G., Shaw, R. A., Thrane, K., Keulen, N.: Europe’s rare earth element resource potential: An overview of REE metallogenetic provinces and their geodynamic setting, Ore Geol. Rev., 72, 838–856, https://doi.org/10.1016/j.oregeorev.2015.09.019, 2016.

Goudie, A. S., Middleton, N. J.: Saharan dust storms: nature and consequences, Earth Sci. Rev., 56, 179–204, https://doi.org/10.1016/S0012-8252(01)00067-8, 2001.

Graedel, T. E., Harper, E. M., Nassar, N. T., Reck, B. K.: Criticality of metals and metalloids, Proceedings of the National Academy of Sciences, 112 4257–4262, https://doi.org/10.1073/pnas.1500415112, 2015.

Gutiérrez, M., Casillas, R., Fernández, C., Balogh, K., Ahijado, A., Castillo, C., Colmenero, J. R., García-Navarro, E.: The submarine volcanic succession of the basal complex of Fuerteventura, Canary Islands: A model of submarine growth and emergence of tectonic volcanic islands, Bulletin of the Geological Society of America, 118, 785–804, https://doi.org/10.1130/B25821.1, 2006.

Gutiérrez-Elorza, M., Lucha, P., Gracia, F. J., Desir, G., Marín, C., Petit-Maire, N.: Palaeoclimatic considerations of talus flatirons and aeolian deposits in Northern Fuerteventura volcanic island (Canary Islands, Spain), Geomorphology, 197, 1–9, https://doi.org/10.1016/j.geomorph.2011.09.020, 2013.

Haxel, G. B.: Ultrapotassic mafic dikes and rare earth element- and barium-rich carbonatite at Mountain Pass, Mojave Desert, southern California: summary and field trip localities, U.S. Geol. Surv. Open-File Rep., 1219. http://pubs.usgs.gov/of/2005/1219/, 2005.

Hobson, A., Bussy, F., Hernández, J.: Shallow-level migmatization of gabbrosin a metamorphic contact aureole, Fuerteventura Basal Complex, Canary Islands, Journal of Petrology, 39, 1025–1037, https://doi.org/10.1093/petroj/39.5.1025, 1998.

Hoernle, K., Tilton, G., Le Bas, M.J., Duggen, S., Garbe-Schönberg, D., Geochemistry of oceanic carbonatites compared with continental carbonatites: Mantle recycling of oceanic crustal carbonate, Contrib. Mineral. Petrol., 142, 520–542, https://doi.org/10.1007/s004100100308, 2002.

Holloway, M. I., Bussy, F.: Trace element distribution among rock-forming minerals from metamorphosed to partially molten basic igneous rocks in a contact aureole (Fuerteventura, Canaries), Lithos, 102, 616–639, https://doi.org/10.1016/j.lithos.2007.07.026, 2008.

Huerta, P., Rodríguez-Berriguete, A., Martín-García, R., Martín-Pérez, A., La-Iglesia-Fernández, A., Alonso-Zarza, A.: The role of climate and eolian dust input in calcrete formation in volcanic islands (Lanzarote and Fuerteventura, Spain), Palaeogeogr. Palaeoclimatol. Palaeoecol., 417, 66–79, https://doi.org/10.1016/j.palaeo.2014.10.008, 2015.

Humphreys-Williams, E.R., Zahirovic, S.: Carbonatites and Global Tectonics, Elements, 17, 339–344, https://doi.org/10.2138/gselements.17.5.339, 2021.

Jahn, R., Blume, H. P., Asio, V. B., Spaargaren, O., Schad, P.: Guidelines for soil description, FAO, Rome 97 p, https://www.fao.org/3/a0541e/a0541e.pdf, 2006.

Jyothi, R. K., Thenepalli, T., Ahn, J. W., Parhi, P. K., Chung, K. W., Lee, J. Y.: Review of rare earth elements recovery from secondary resources for clean energy technologies: grand opportunities to create wealth from waste, J. Clean. Prod., 267, 122048, https://doi.org/10.1016/j.jclepro.2020.122048, 2020.

Kamenetsky, V.S., Doroshkevich, A.G., Elliot, H.A.L., Zaitsev, A.N., Carbonatites: Contrasting, Complex, and Controversial, Elements, 17, 307–314, https://doi.org/10.2138/gselements.17.5.307, 2021.

Kravchenko, S. M., Pokrovsky, B. G.: The Tomtor alkaline ultrabasic massif and related REE-Nb deposits, northern Siberia, Economic Geology, 90, 676–689, https://doi.org/10.2113/gsecongeo.90.3.676, 1995.

Kravchenko, S. M., Czamanske, G., Fedorenko, V. A.: Geochemistry of carbonatites of the Tomtor massif, Geochem. Int., 41, 545–558, ISSN: 0016-7029, 2003.

Lai, X., Yang, X., Santosh, M., Liu, Y., Ling, M.: New data of the Bayan Obo Fe-REE-Nb deposit, Inner Mongolia: Implications for ore gènesis, Precambrian Research, 263, 108–122, https://doi.org/10.1016/j.precamres.2015.03.013, 2015.

Le Bas, M. J.: The pyroxenite-ijolite-carbonatite intrusive igneous complexes of Fuerteventura, Canary Islands, J. Geol. Soc. London, 138, 496, https://doi.org/10.1144/gsjgs.138.4.0493, 1981.

Le Bas, M. J, Rex, D. C., Stillman, C. J.: The early magmatic chronology of Fuerteventura, Geol. Mag., 123, 287–298, https://doi.org/10.1017/S0016756800034762, 1986.

Le Maitre, R.W., Igneous Rocks: a Classification and Glossary of Terms, Cambridge University Press, Cambridge, U.K, 2002.

Le Maitre, R. W., Streckeisen, A., Zanettin, B., Le Bas, M. J., Bonin, B., Bateman, P., Bellieni, G., Dudek, A., Efremova, S., Keller, J., Lameyre, J., Sabine, P. A., Schmid, R., Sorensen, H., Woolley, A. R.: Igneous Rocks: A Classification and Glossary of Terms, 2nd Edition, Cambridge, UK, Cambridge Univ. Press, ISBN: 9780521619486, 2005.

Liu, Y. L., Ling, M. X., Williams, I. S., Yang, X. Y., Wang, C. Y., Sun, W.: The formation of the giant Bayan Obo REE-Nb-Fe deposit, North China, Mesoproterozoic carbonatite overprinted Paleozoic dolomitization, Ore Geology Reviews, 92, 73–83, https://doi.org/10.1016/j.oregeorev.2017.11.011, 2018.

Long, K. R., Van Gosen, B. S., Foley, N. K., Cordier, D.: The principal rare earth elements deposits of the United States: A summary of domestic deposits and a global perspective, https://pubs.usgs.gov/sir/2010/5220/, 2010.

Longpré, M. A., Felpeto, A.: Historical volcanism in the Canary Islands; part 1: A review of precursory and eruptive activity, eruption parameter estimates, and implications for hazard assessment, Journal of Volcanology and Geothermal Research, 419, 107363, https://doi.org/10.1016/j.jvolgeores.2021.107363, 2021.

Machado-Yanes, M. C.: Reconstrucción paleoecológica y etnoarqueológica por medio del análisis antracológico.La Cueva de Villaverde, Fuerteventura, In: Biogeografía Pleistocena-Holocena de la Península Ibérica, 261274, Ramil-Rego, P., Fernández-Rodríguez, C., Rodríguez-Guitián, M. (Eds.), ISBN 84-453-1716-4, 261 p, 1996.

Mangas, J., Pérez-Torrado, F. J., Reguillón, R. M., Cabrera, M. C.: Prospección radiométrica en rocas alcalinas y carbonatitas de la serie plutónica I de Fuerteventura (Islas Canarias). Resultados preliminares e implicaciones metalogénicas, Actas del III Congreso Geológico de España y VIII Congreso Latinoamericano de Geología. Salamanca, 3, 389–393, ISBN: 84-600-8114-1, 1992.

Mangas, J., Pérez-Torrado, F. J., Reguillón, R. M., Martin-Izard, A.: Mineralizaciones de tierras raras ligadas a los complejos intrusivos alcalino-carbonatíticos de Fuerteventura (Islas Canarias), Bol. Soc. Esp. Min., 17, 212–213, 1994.

Mangas, J., Pérez-Torrado, F. J., Reguillón, R. M., Martin-Izard, A.: Rare earth minerals in carbonatites of Basal Complex of Fuerteventura (Canary Islands, Spain), In: Mineral Deposit: Research and

Exploration, where do they meet? Ed. Balkema, Rotterdam, 475–478, ISBN-13: 978-9054108894, 1997.

Mariano, A. N., Mariano, Jr. A.: Rare earth mining and exploration in North America, Elements, 8, 369–376, https://doi.org/10.2113/gselements.8.5.369, 2012.

Massari, S., Ruberti, M.: Rare earth elements as critical raw materials: Focus on international markets and future strategies, Resour. Policy, 38, 36–43, https://doi.org/10.1016/j.resourpol.2012.07.001, 2013.

McDonough, W., Sun, W.: The composition of the Earth, Chemical Geology, 67, 1050–1056, https://doi.org/10.1016/0009-2541(94)00140-4, 1995.

Méndez-Ramos, J., Acosta-Mora, P., Ruiz-Morales, J. C., Hernández, T., Morge, M. E., Esparza, P.: Turning into the blue: materials for enhancing TiO_2 photocatalysis by up-conversion photonics, RSC Advances, 3, 23028–23034, https://doi.org/10.1039/C3RA44342F, 2013.

Menéndez, I., Díaz-Hernández, J. L., Mangas, J., Alonso, I., Sánchez-Soto, P. J.: Airborne dust accumulation and soil development in the North-East sector of Gran Canaria (Canary Islands, Spain), J. Arid Environ., 71, 57–81, https://doi.org/10.1016/j.jaridenv.2007.03.011, 2007.

Menéndez, I., Campeny, M., Quevedo-González, L., Mangas, J., Llovet, X., Tauler, E., Barrón, V., Torrent, J., Méndez-Ramos, J.: Distribution of REE-bearing minerals in felsic magmatic rocks and paleosols from Gran Canaria, Spain: Intraplate oceanic islands as a new example of potential, non-conventional sources of rare-earth elements, Journal of Geochemical Exploration, 204, 270–288, https://doi.org/10.1016/j.gexplo.2019.06.007, 2019.

Moore, M., Chakhmouradian, A., Mariano, A. N., Sidhu, R.: Evolution of Rare-earth Mineralization in the Bear Lodge Carbonatite, In: Ore Geology Reviews, 64, Mineralogical and Isotopic Evidence, Wyoming, 499, 521, http://dx.doi.org/10.1016/j.oregeorev.2014.03.015, 2015.

Mourão, C., Mata, J., Doucelance, R., Madeira, J., da Silveira, A.B., Silva, L.C., Moreira, M., Quaternary extrusive calciocarbonatite volcanism on Brava Island (Cape Verde): A nephelinite-carbonatite immiscibility product, Journal of African Earth Sciences, 56, 59–74, https://doi.org/10.1016/j.jafrearsci.2009.06.003, 2010.

Muñoz, M.: Ring complexes of Pájara in Fuerteventura Island, Bulletin Volcanologique, 33, 840–861, https://doi.org/10.1007/BF02596753, 1969.

Muñoz, M., Sagredo, J., de Ignacio, C., Fernández-Suárez, J., Jeffries, T. E.: New data (U-Pb, K-Ar) on the geochronology of the alkaline-carbonatitic association of Fuerteventura, Canary Islands, Spain, Lithos, 85, 140–153, https://doi.org/10.1016/j.lithos.2005.03.024, 2005.

Olson, J.C., Shawe, D. R., Pray, L.C., Sharp, W. N.: Rare-Earth Mineral Deposits of the Mountain Pass District, San Bernardino County, California, Science, 119, 325–326, https://doi.org/10.1126/science.119.3088.325, 1954.

Park, J., Rye, D.M., Broader Impacts of the Metasomatic Underplating Hypothesis, Geochem. Geophys. Geosyst., 20, 4180–4829, https://doi.org/10.1029/2019GC008493, 2019.

Pérez-Torrado, F. J., Carracedo, J. C., Guillou, H., Rodríguez-González, A., Fernández-Turiel, J. L.: Age, duration, and spatial distribution of ocean shields and rejuvenated volcanism: Fuerteventura and Lanzarote, Eastern Canaries, Journal of the Geological Society of London, 180, https://doi.org/10.1144/jgs2022-112, 2023.

Pirajno, F., Yu, H.C.: The carbonatite story once more and associated REE mineral systems, Gondwana Research, 107, 281–295. https://doi.org/10.1016/j.gr.2022.03.006, 2022.

Reinhardt, N., Proenza, J., Villanova-de-Benavent, C., Aiglsperger, T., Bover-Arnal, T., Torró, L., Salas, R., Dziggel, A.: Geochemistry and Mineralogy of Rare Earth Elements (REE) in Bauxitic Ores of the Catalan Coastal Range, NE Spain, Minerals, 8, 562, https://doi.org/10.3390/min8120562, 2018.

Rudnick, R.L., Gao, S.: Composition of the Continental Crust, In: Holland, H.H., Turekian, K.K. (editors): Treatise on Geochemistry, 4, 1–51, https://doi.org/10.1016/B978-0-08-095975-7.00301-6, 2014.

Scheuvens, D., Schütz, L., Kandler, K., Ebert, M., Weinbruch, S.: Bulk composition of northern African dust and its source sediments—a compilation, Earth Sci. Rev., 116, 170–194, https://doi.org/10.1016/j.earscirev.2012.08.005, 2013.

Schmincke, H., Sumita, M.: Geological evolution of the Canary Islands: a young volcanic archipelago adjacent to the old African Continent, Ed. Görres, Koblenz, 200 p, ISBN: 978-3-86972-005-0, 2010.

Smith, M. P., Campbell, L. S., Kynicky, J.: A review of the genesis of the world class Bayan Obo Fe-REE-Nb deposits, Inner Mongolia, China: multistage processes and outstanding qüestions, Ore Geology Reviews, 64, 459–476, https://doi.org/10.1016/j.oregeorev.2014.03.007, 2015.

Smith, M. P., Moore, K., Kavecsánszki, D., Finch, A. A., Kynicky, J., Wall, F.: From mantle to critical zone: A review of large and giant-sized deposits of the rare earth elements, Geoscience Frontiers, 7, 315–334, https://doi.org/10.1016/j.gsf.2015.12.006, 2016.

Steiner, C., Hobson, A., Favre, P., Stampli, G. M.: Early Jurassic sea-floor spreading in the central Atlantic — the Jurassic sequence of Fuerteventura (Canary Islands), Geological Society of American Bulletin, 110, 1304–1317, https://doi.org/10.1130/0016-7606(1998)110<1304:MSOFCI>2.3.CO;2, 1998.

Torró, L., Proenza, J. A., Aiglsperger, T., Bover-Arnal, T., Villanova-de-Benavent, C., Rodríguez-García, D., Ramírez, A., Rodríguez, J., Mosquea, L.A., Salas, R.: Geological, geochemical and mineralogical characteristics of REE-bearing Las Mercedes bauxite deposit, Dominican Republic, Ore Geol. Rev., 89, 114–131, https://doi.org/10.1016/j.oregeorev.2017.06.017, 2017.

Torró, L., Villanova, C., Castillo, M., Campeny, M., Gonçalves, A. O., Melgarejo, J. C.: Niobium and rare earth minerals from the Virulundo carbonatite, Namibe, Angola, Mineralogical Magazine, 76, 393–409, https://doi.org/10.1180/minmag.2012.076.2.08, 2012.

Troll, V., Carracedo, J. C.: The Geology of Fuerteventura, In: Troll, V., Carracedo, J. C., Weismaier, S. (eds), The Geology of Canary Islands, Elsevier, 531–582. http://dx.doi.org/10.1016/B978-0-12-809663-5.00008-6, 2016.

van den Bogaard, P.: The origin of the Canary Island Seamount Province - New ages of old seamounts, Scientific Reports, 3, 2107. https://doi.org/10.1038/srep02107, 2013.

Wang, Q., Deng, J., Liu, X., Zhang, Q., Sun, S., Jiang, C., Zhou, F.: Discovery of the REE minerals and its geological significance in the Quyang bauxite deposit, West Guangxi, China, J. Asian Earth Sci., 39, 701–712, https://doi.org/10.1016/j.jseaes.2010.05.005, 2010.

Wang, X., Jiao, Y., Du, Y., Ling, W., Wu, L., Cui, T., Zhou, Q., Jin, Z., Lei, Z., Wen, S.: REE mobility and Ce anomaly in bauxite deposit of WZD area, Northern Guizhou, China, J. Geochem Explor., 133, 103–117, https://doi.org/10.1016/j.gexplo.2013.08.009, 2013.

Wang, Z.Y., Fan, H.R., Zhou, L., Yang, K.F., She, H.D., Carbonatite-related REE deposits: An overview, Minerals, 10, 965. https://doi.org/10.3390/min10110965, 2020.

Warr, L. N.: IMA–CNMNC approved mineral symbols, Mineralogical Magazine, 85, 291–320, https://doi.org/10.1180/mgm.2021.43, 2021.

Weidendorfer, D., Schmidt, M.W., Mattsson, H.B.: Fractional crystallization of Si-undersaturated alkaline magmas leading to unmixing of carbonatites on Brava Island (Cape Verde) and a general model of carbonatite genesis in alkaline magma suites, Contributions to Mineralogy and Petrology, 171, 43, https://doi.org/10.1007/s00410-016-1249-5, 2016.

Wondraczek, L., Tyystjärvi, E., Méndez-Ramos, J., Müller, F. A., Zhang. Q.: Shifting the Sun: Solar Spectral Conversion and Extrinsic Sensitization in Natural and Artificial Photosynthesis, Advanced Science, 2, 1500218, https://doi.org/10.1002/advs.201500218, 2015.

Woolley, A.R., Kjarsgaard, B.A. (2008): Carbonatites of the world: map and database. Mineralogical Magazine 71, 718.

Wu, C.: Bayan Obo Controversy: Carbonatites versus Iron Oxide-Cu-Au-(REE-U), Resource Geology, 58, 348–354, https://doi.org/10.1111/j.1751-3928.2008.00069.x, 2008.

Yang, K., Fan, H., Pirajno, F., Li, X.: The bayan Obo (China) giant REE accumulation conundrum elucidated by intense magmatic differentiation of carbonatite, Geology, 47, 1198–1202, https://doi.org/10.1130/G46674.1, 2019.

Yaxley, G.M., Anenburg, M., Tappe, S., Decree, S., Guzmics, T.: Carbonatites: Classification, Sources, Evolution, and Emplacement, Annual Reviews on Earth and Planetary Sciences, 50, 261–293, https://doi.org/10.1146/annurev-earth-032320-104243, 2022.

Zazo, C., Goy, J. L., Hillaire-Marcel, C., Gillot, P. Y., Soler, V., González, J. A., Dabrio, C. J., Ghaleb, B.: Raised marine sequences of Lanzarote and Fuerteventura revisited –a reappraisal of relative sea-level changes and vertical movements in the eastern Canary Islands during the Quaternary, Quaternary Science Reviews, 21, 2019–2046, https://doi.org/10.1016/S0277-3791(02)00009-4, 2002.

Zhukova, I. A., Stepanov, A. S., Jiang, S. Y., Murphy, D., Mavrogenes, J., Allen, C., Chen, W., Bottrill, R.: Complex REE systematics of carbonatites and weathering products from uniquely rich Mount Weld REE deposit, Western Australia, Ore Geology Reviews, 139, 104539, https://doi.org/10.1016/j.oregeorev.2021.104539,2021.

Figure 1

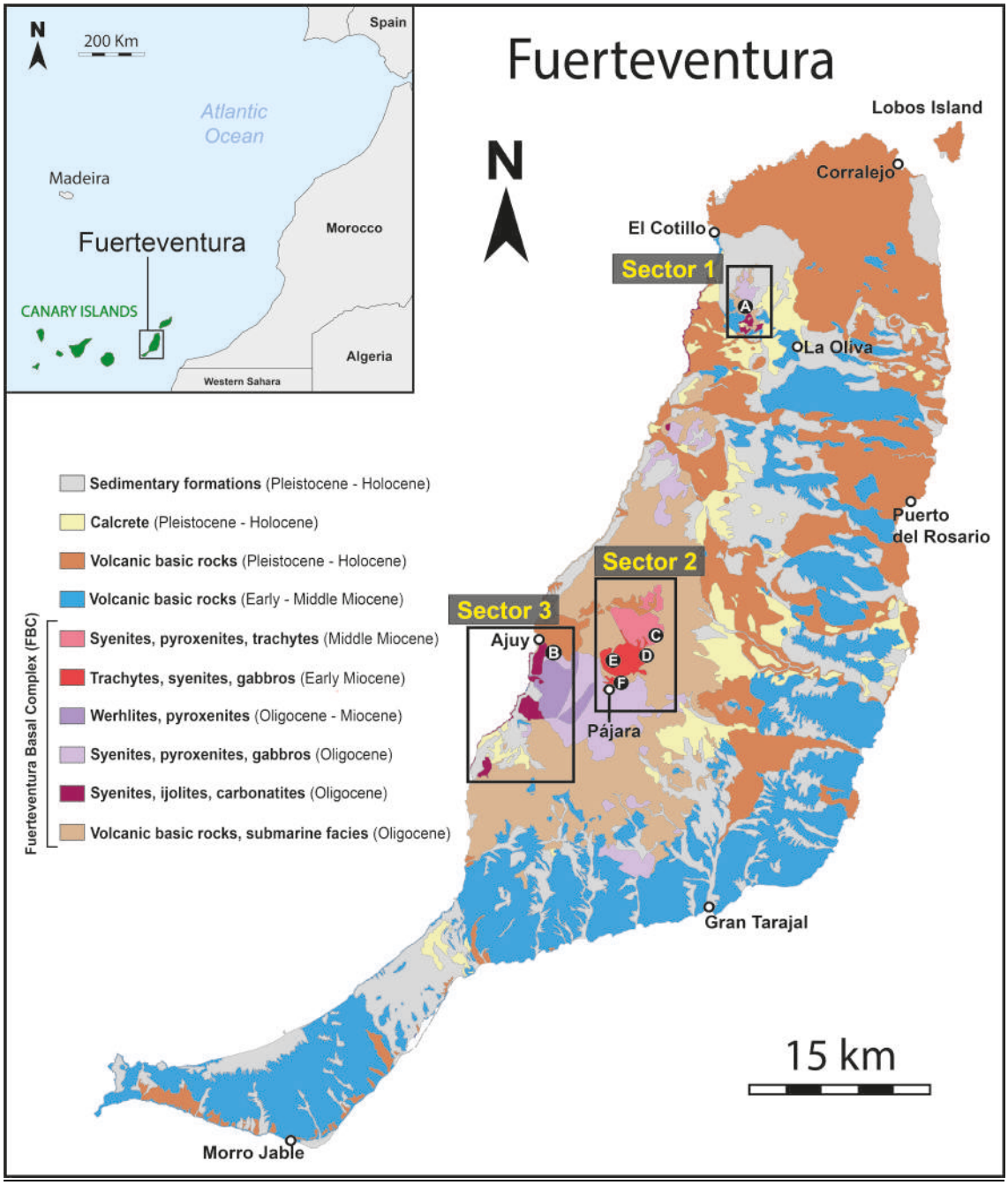

Figure 1: Simplified geological map of Fuerteventura Island (modified from Balcells et al., 2006) showing the location of the three study sectors for the assessment of REE content in the FBC. Additionally, the studied weathering profiles are also indicated, as: (A) Agua Salada ravine; (B) Aulagar ravine; (C) Palomares ravine; (D) FV-30 road; (E) Las Peñitas quarry; (F) Pájara.

Figure 2

Figure 2: (a), **(b)** Images showing typical outcrops of the FBC in the southern area of Ajuy (sector 3; Figure 1). The images highlight characteristic swarms of alkaline and carbonatitic intrusions (whitish) intersected by later-intruded basaltic dikes (black colour). **(c)** Detailed view of a carbonatitic dike located in a shear zone of sector 3, exhibiting distinct linear sigmoidal structures resulting from deformation. **(d)** Detailed view of centimetre-sized phlogopite crystals within a carbonatitic dike outcropping in sector 3, displaying a typical pegmatitic texture. **(e)** Overview of an outcrop of metric-scale carbonatitic dikes in the sector 1 area.

Figure 3

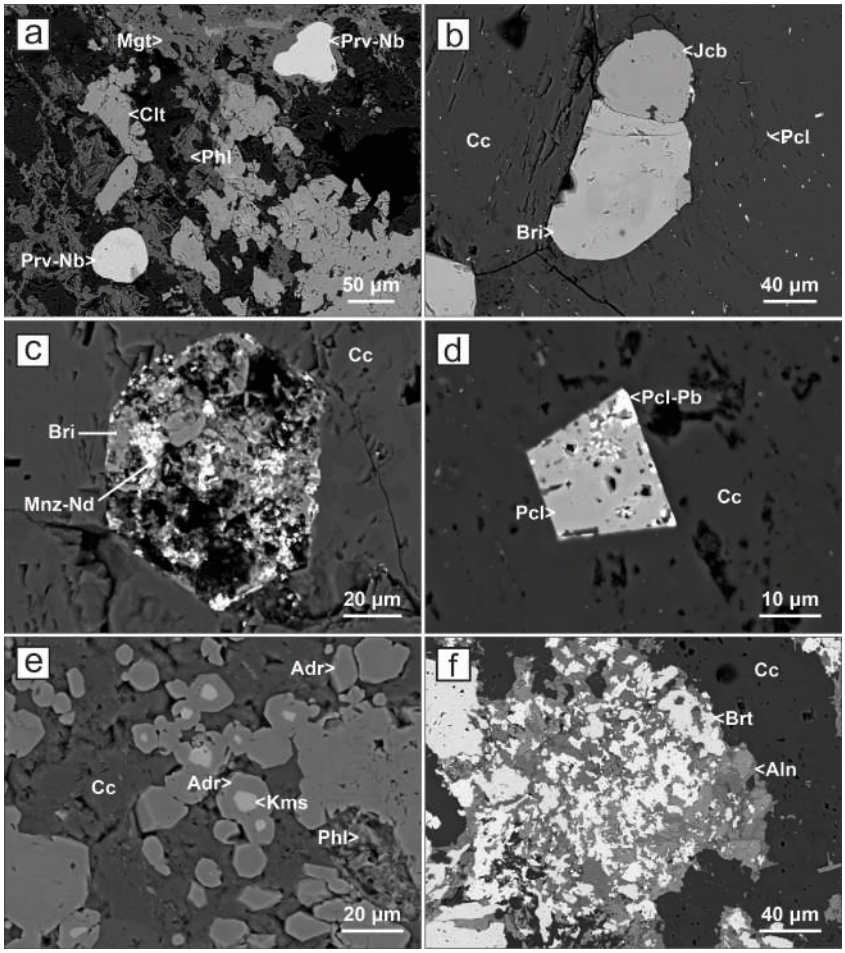

Figure 3: SEM (backscattered electron, BSE) images of the Fuerteventura carbonatites. **(a)** Subhedral crystals of niobium-rich perovskite (Prv-Nb) associated with phlogopite (Phl) and magnetite (Mgt) aggregates. The association has been affected by secondary hydrothermal processes, leading to the formation of celestine (Clt). **(b)** Typical subhedral crystal of jacobsite (Jcb) associated with britholite (Bri). Both crystals are hosted in magmatic calcite (Cc), with numerous disseminated microcrystals of pyrochlore (Pcl). **(c)** Partially altered subhedral grain of britholite (Bri) hosted in magmatic calcite (Cc). The alteration process led to the formation of secondary REE phosphates such as monazite-Nd (Mnz-Nd). **(d)** Euhedral crystal of pyrochlore (Pcl) hosted in calcite (Cc). Brighter areas developed on the grain's borders correspond to plumbopyrochlore (Pcl-Pb) zonation. **(e)** Typical mineral association related to small skarn like areas associated with carbonatites. Subhedral zoned crystals of andradite (Adr), hosted in calcite (Cc) and phlogopite (Phl), with a significant Zr zoning leading to kerimasite (Kms) cores. **(f)** Typical low-metamorphic alteration developed on carbonatites composed of allanite (Aln) aggregates hosted in calcite (Cc) and associated with secondary baryte (Brt). Abbreviations of mineral names in all the pictures follow the criteria proposed by Warr (2021).

928 **Figure 4**

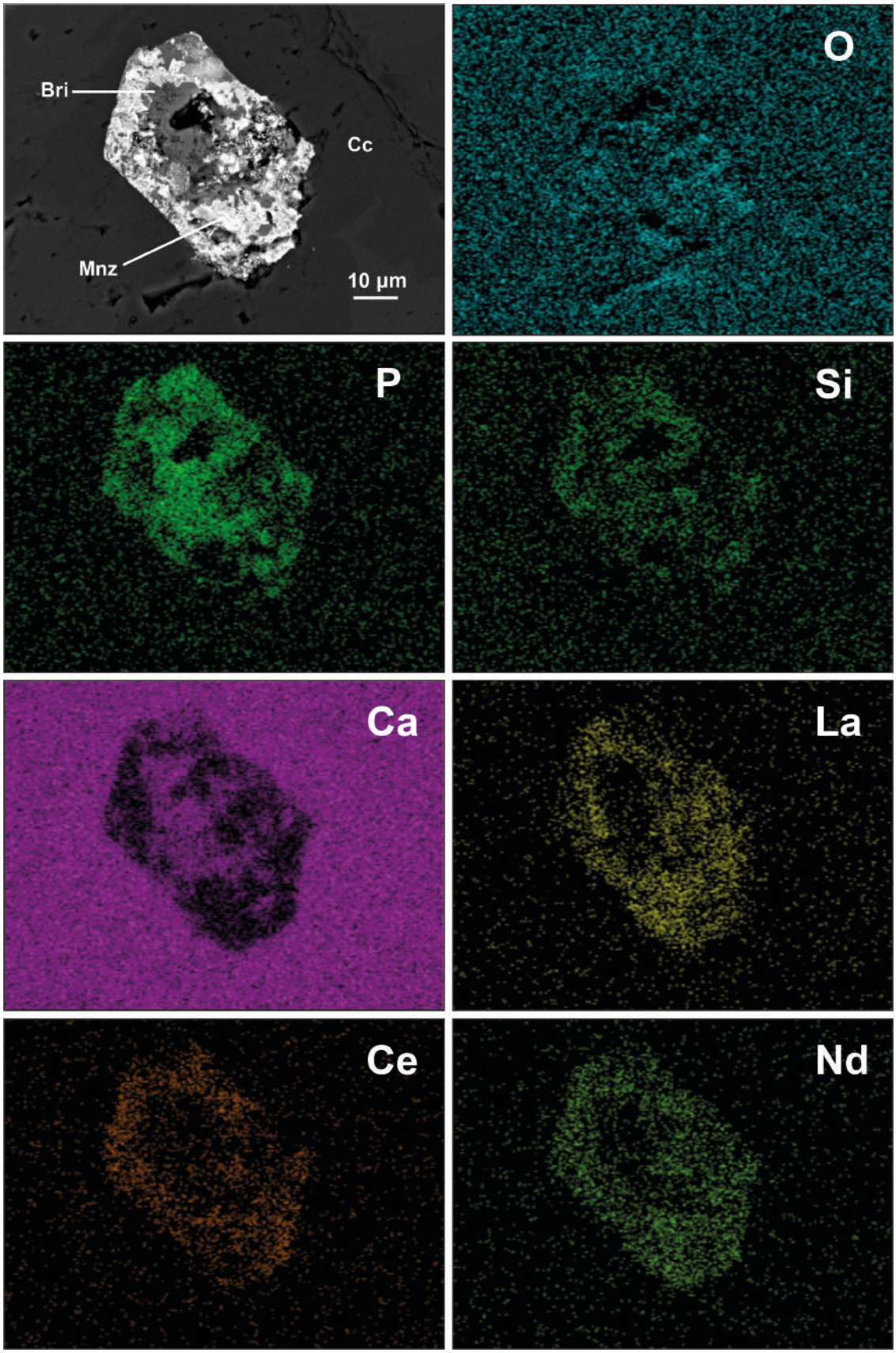

929

930 **Figure 4:** Wavelength-dispersive X-ray maps of representative compositional elements for an altered grain

931 of britholite (Bri) hosted in calcite (Cc) and partially transformed into secondary monazite (Mnz).

Figure 5

Figure 5: **(a)** General view of a typical surface outcrop of Quaternary calcrete located in the Aulagar ravine area (profile B, sector 3; Fig.1). **(b)** Centimetre-thick calcrete layer filling a fracture between two carbonatitic dikes in the Aulagar ravine area (profile B, sector 3; Fig.1). **(c)** Calcrete layer developed within fractures between carbonatitic rocks in the Agua Salada ravine area (profile A, sector 1; Fig.1).

Figure 6

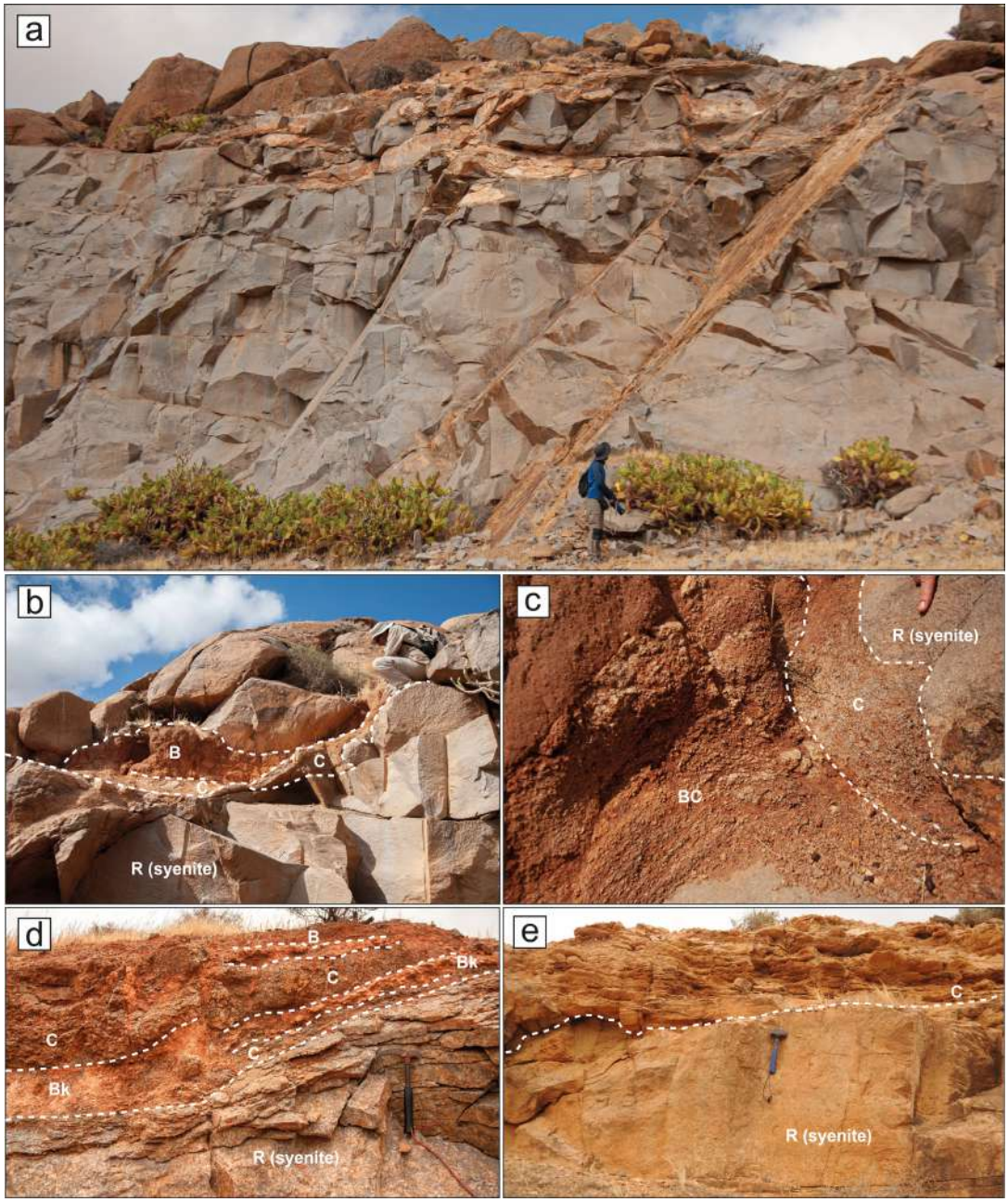

Figure 6: (a) General view of Las Peñitas quarry syenite outcrop (profile E, sector 2; Fig.1) where it is possible to distinguish different fractures filled by injected secondary weathering products. **(b)** Syenite weathering profile in Las Peñitas quarry (profile E, sector 2; Figure 1) showing surface erosion and B, BC and C horizons injected in the syenite bedrock (R). **(c)** Weathering profile displaying the development of C and BC horizons associated with a syenite protolith (R), located in Las Peñitas quarry (profile E, sector 2; Figure 1). **(d)** Weathering profile developed on syenite in the FV-30 road area (profile D, sector 2), exhibiting the development of C, B and calcrete (Bk) horizons. **(e)** Weathering profile on syenite protolith (R) displaying a metric sized C horizon in the Pájara area (profile F, sector 2; Figure 1).

960 **Figure 7**

961 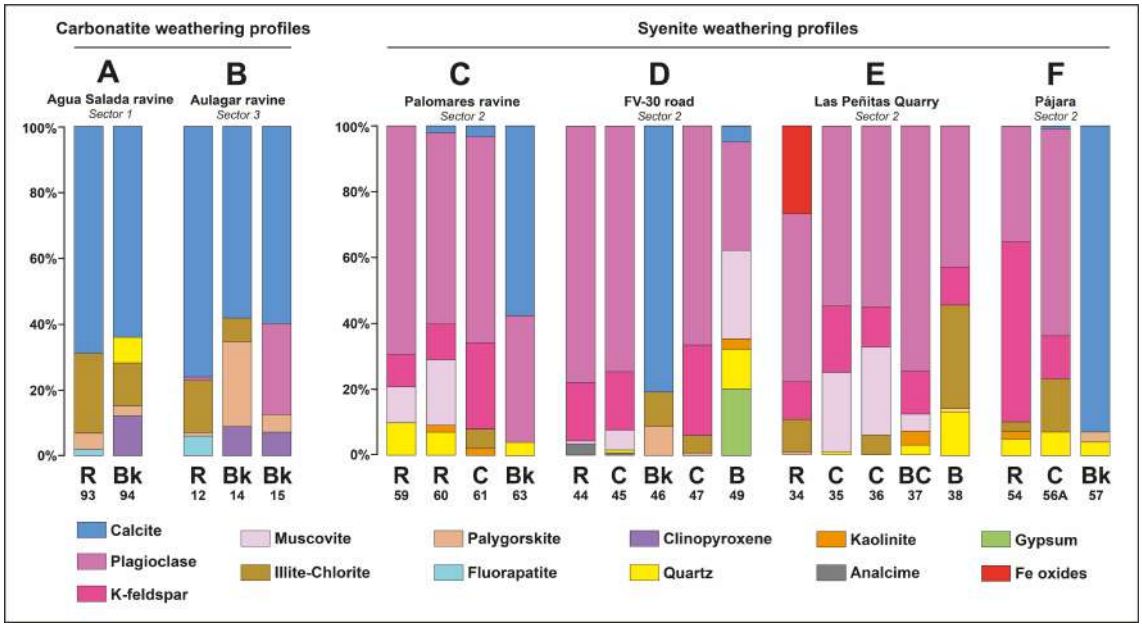

962 **Figure 7**: Graphical mineralogical quantification of the studied weathering profiles: (A) Agua Salada
963 ravine; (B) Aulagar ravine; (C) Palomares ravine; (D) FV-30 road; (E) Las Peñitas quarry; (F) Pájara. The
964 corresponding class assigned to the edaphic horizons (B, BC, Bk, C, R) and the sample number are shown
965 at the foot of the columns.

966
967
968
969
970
971
972
973
974
975
976
977
978
979
980
981

Figure 8

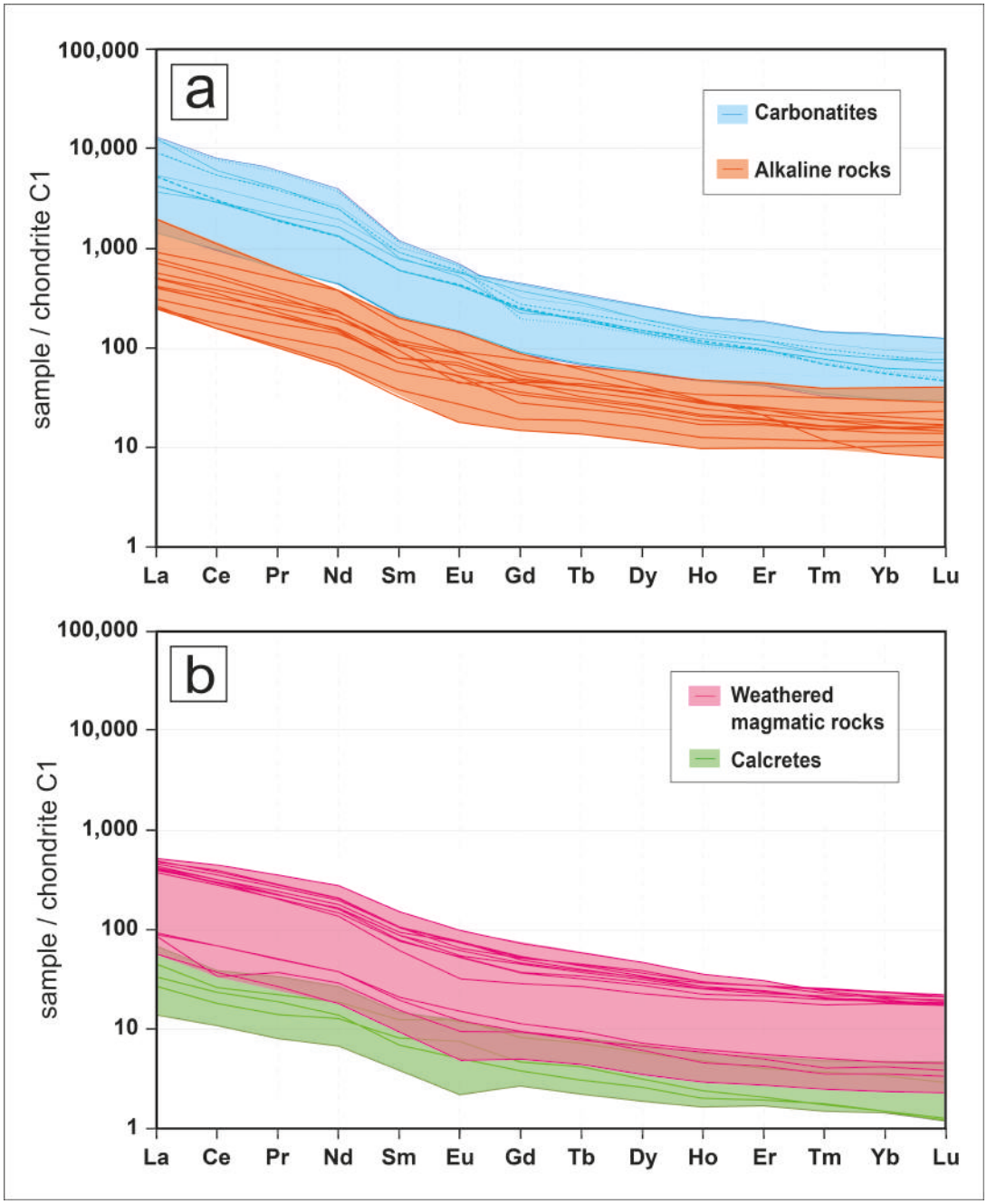

Figure 8: REE plots of the studied Fuerteventura lithologies normalised to C1 chondrites. Normalisation values are from McDonough and Sun (1995).

Figure 9

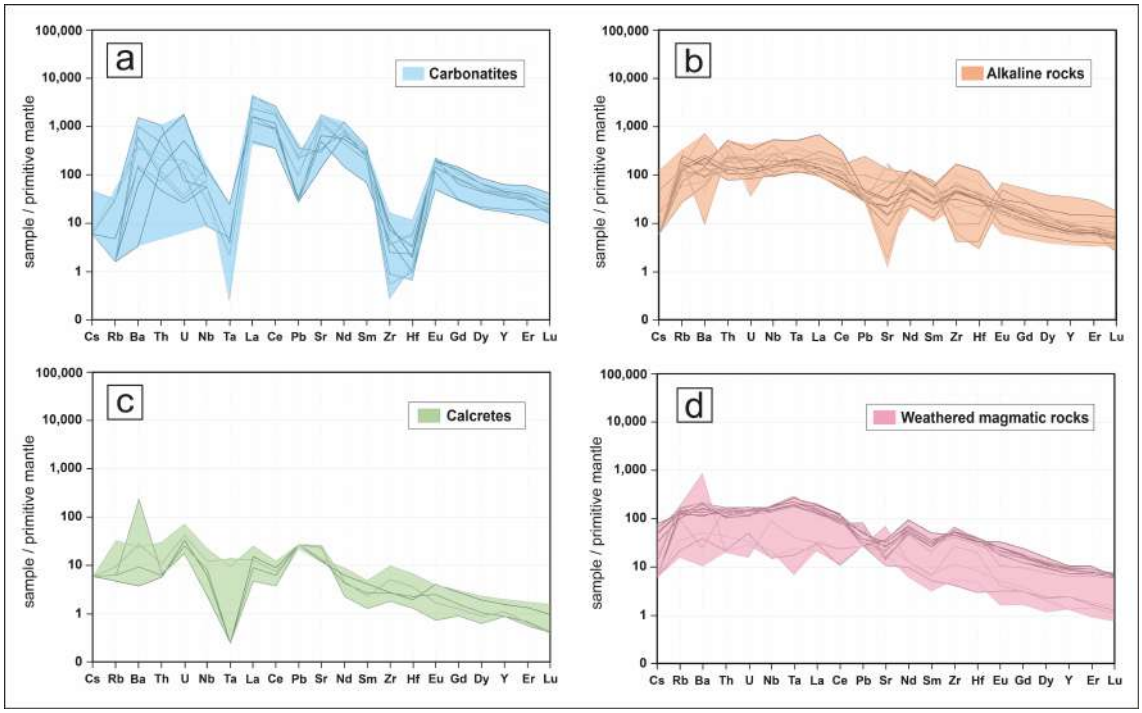

Figure 9: Multi-elemental trace element plots of Fuerteventura intrusive lithologies normalised to the primitive mantle. Normalisation values from McDonough and Sun (1995).

Figure 10

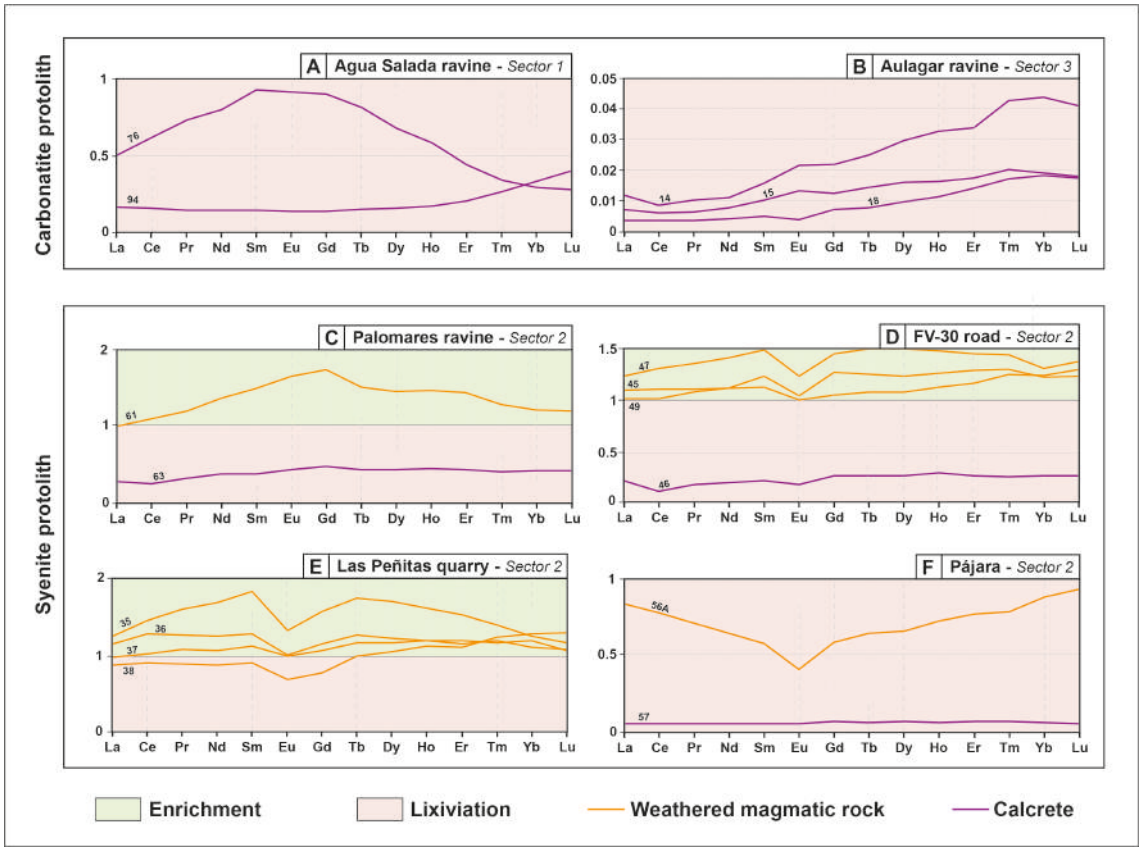

Figure 10: REE weathering enrichment/leaching diagrams between primary magmatic protoliths (carbonatites and syenites) and the associated weathering products from the studied profiles (Figure 1). The sample number is labelled on the corresponding pattern line.

Figure 11

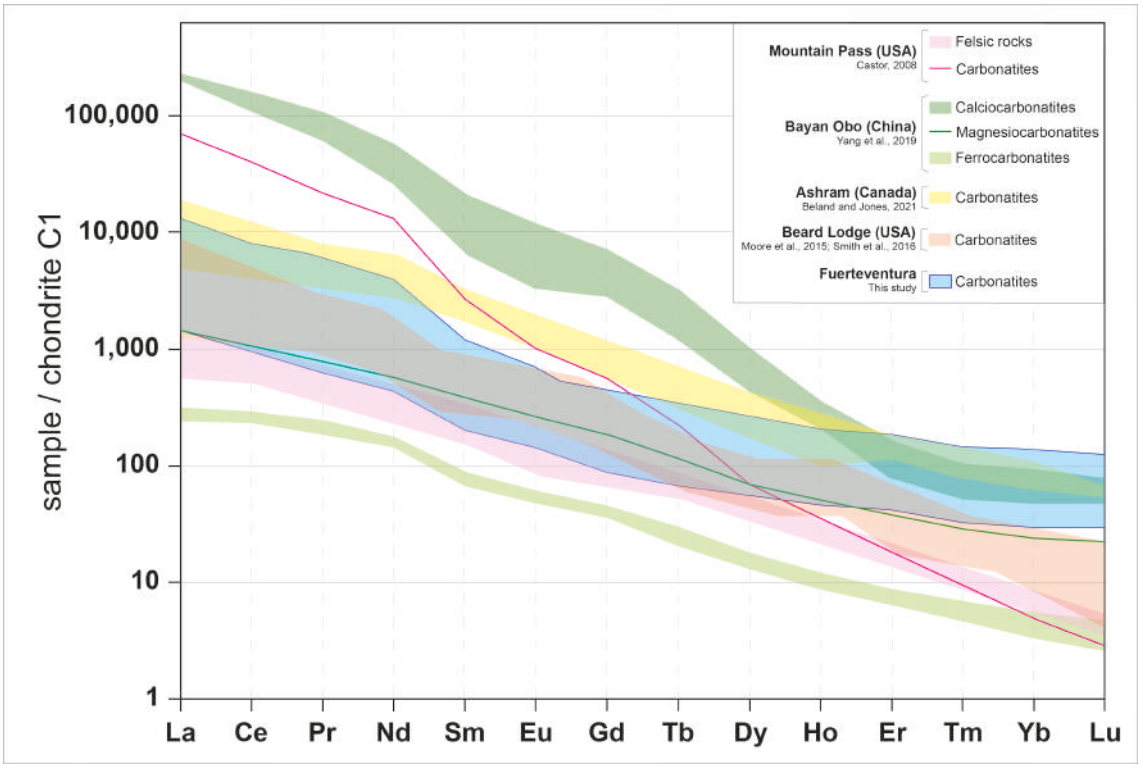

Figure 11: REE plot of the studied Fuerteventura carbonatites compared to other carbonatitic localities worldwide where REE deposits have been reported. REE contents for comparison are from Castor (2008), Yang et al. (2019), and Beland and Jones (2021). Normalisation values are from McDonough and Sun (1995).